High JNK following Ras/Rpr/Tak1 over-expression in imaginal discs of *Drosophila* reduces post-pupariation ecdysone via Dilp8 resulting in early pupal death

Mukulika Ray and Subhash C. Lakhotia*

Cytogenetics Laboratory, Department of Zoology, Banaras Hindu University, India 221005

* Author for correspondence (Orcid no. 0000-0003-1842-8411)
Email: lakhotia@bhu.ac.in

Orcid ID:
Mukulika Ray: orcid.org/0000-0002-9064-818X
S. C. Lakhotia: orcid.org/0000-0003-1842-8411

Tele: +91-542-2368146

Running title: Dilp8 and early pupal death

Abstract

We examined reasons for early pupal death following expression of certain transgenes with predominantly eye- (*GMR-GAL4* or *sev-GAL4*) or wing- (*MS1096-GAL4*) disc specific drivers. The *GMR-GAL4>UAS-Ras1*^{V12} expression or co-expression of *sev-GAL4>UAS-Ras1*^{V12} and *UAS-hsrω-RNAi* transgene or *EP3037* to down or up-regulate, respectively, the *hsrω* lncRNAs caused early (~25-30 Hr after pupa formation, APF) pupal death, with absence of the normal 8-12 Hr APF ecdysone surge. Exogenous ecdysone between 8-20 Hr APF partially suppressed the early death. Similar early pupal death was also seen following *GMR-GAL4>*driven *UAS-tak1* expression or *MS1096-GAL4* driven Ras/JNK activation. Genotypes showing early pupal death displayed increase in some JNK pathway members, and Dilp8 in late larval and more so in early pupal eye discs, reduced transcripts of *ptth* in brain lobes and of ecdysone biosynthesis enzymes in prothoracic glands of 8-9 Hr old pupae. High JNK activity in late larval imaginal discs triggers greater Dilp8 secretion from them soon after pupa formation, which inhibits post-pupal ecdysone synthesis in prothoracic gland, leading to early pupal death. This highlights how mis-regulated signaling in one tissue can have global deleterious consequences through downstream events in other tissues, reemphasizing roles of inter-organ signaling in life of an organism.

Keywords: pMAPK, JNK, Tak1-like 1, Halloween genes, , *hsrω* lncRNA

Introduction

Several earlier studies reported pupal lethality following *GMR-GAL4* or *sev-GAL4* expression of certain transgenes (Mallik and Lakhotia, 2009b; Morris et al., 2006) (Ray and Lakhotia, 2017). Pupal lethality following transgene expression under these two mostly eye-specific GAL4 drivers (Bowtell et al., 1991; Firth et al., 2006; Freeman, 1996; Maixner et al., 1998) is intriguing since even a complete absence of eyes does not affect viability of pupae and adult fly emergence (Sang and Jackson, 2005). Our recent finding (Ray and Lakhotia, 2015) that besides the well-known expression in eye disc cells, the *GMR-GAL4* and *sev-GAL4* drivers also express in several other cell types including specific neurons in the central nervous system (CNS) raised the possibility that transgene's ectopic expression in some of these other cells may cause pupal death. We examined these possibilities in the present study and found that expression of different transgenes by predominantly eye- or wing-disc specific GAL4 drivers that lead to high JNK activity in late larval imaginal discs elevate Dilp8 in early pupal discs, which in turn reduced *ptth* transcripts in early pupal brain lobes and consequently of some Halloween genes like *phantom* and *spok* in prothoracic gland. Together, these changes disrupt post-pupariation ecdysone synthesis, leading to early pupal death. Earlier reports (Colombani et al., 2012; Garelli et al., 2012) showed that damaged or inappropriately growing imaginal discs secrete Dilp8, one of the eight insulin-like signal peptides in *Drosophila* (Nässel et al., 2013), to delay metamorphosis by inhibiting ecdysone synthesis (Colombani et al., 2012; Garelli et al., 2012). Our study shows for the first time that Dilp8 may also be induced by ectopic Ras signaling, affecting ecdysone signaling even at pupal stage. It thus highlights that changes in signaling cascade in one cell type (epithelia) can regulate downstream events in cells of completely different lineage (brain and prothoracic gland) emphasizing significance of inter-organ communications that maintains cellular and organismal homeostasis or trigger death. Early results of this study were published as pre-print (Ray and Lakhotia, 2016 preprint).

Results

Expression of activated Ras in eye imaginal discs caused early/late pupal lethality

We used the predominantly eye specific *sev-GAL4* and *GMR-GAL4* drivers to express the *UAS-Ras1^{V12}* transgene which produces activated Ras and thus triggers the downstream signaling cascade without the need for ligand binding (Karim et al., 1996). Unlike the *sev-GAL4* expression in a few photoreceptor cells in each ommatidium of eye discs, the *GMR-GAL4* expression is seen in nearly all cells of the eye disc behind the morphogenetic furrow (Ray and Lakhotia, 2015). The *sev-GAL4* driven expression of *UAS-Ras1^{V12}* resulted in late pupal lethality while the *GMR-GAL4>UAS-Ras1^{V12}* expression caused 100% early pupal lethality with developmental defects setting in by 8-9 Hr after pupa formation (APF) stage. As reported earlier (Ray and Lakhotia, 2017), the *sev-GAL4>UAS-Ras1^{V12}* pupae developed normally like wild type (Fig. 1A, E and I) till mid-pupal stages but a majority (~88%, N =1058) of them died subsequently (Fig. 1B, F and J); the remaining pupae eclosed with rough eyes due to the extra R7 photoreceptors. Interestingly, when levels of *hsrω* gene transcripts, known to interact and

enhance Ras signaling (Ray and Lakhotia 1997, Ray and Lakhotia 2017) were lowered by co-expression of *UAS-hsrω-RNAi* transgene (Mallik and Lakhotia, 2009b) in *sev-GAL4>UAS-Ras1^{V12}* expressing pupae, development appeared normal till 8-9 Hr APF (Fig. 1C, G and K) but further development was affected and ~ 96% (N =1177; (Ray and Lakhotia, 2017)) pupae died by 25-30 Hr APF; the few survivors died as late pupae. Following co-expression of the *EP3037* over-expressing allele of *hsrω* (Mallik and Lakhotia, 2009b) with *sev-GAL4>UAS-Ras1^{V12}*, 42% (N =1109) (Ray and Lakhotia, 2017) died by ~25-30 Hr APF and the rest as late pupae (Fig. 1D, H and L). As we have shown elsewhere (Ray and Lakhotia, 2017), the early pupal death of *UAS-hsrω-RNAi* and *sev-GAL4>UAS-Ras1^{V12} EP3037* correlates with the substantially elevated Ras signaling due to complex regulatory interactions between down- or up-regulated *hsrω* lncRNA levels and ectopically enhanced activated Ras expression. Anterior part of all early dying pupae appeared empty with necrotic patches near eye region appearing by 23-24 Hr APF (Fig. 1K and L). Although they showed demarcation between head, thorax and abdomen, Malpighian tubules (MT), which become abdominal by this stage in *sev-GAL4>UAS-Ras1^{V12}* and in wild type (Fig. 2A), remained thoracic (Fig. 2B, C) and retained a comparatively longer anterior segment (Fig. 2E and F) like that in 14-15 Hr old *sev-GAL4>UAS-Ras1^{V12}* or wild type (not shown) pupae. Their cells were far less compactly arranged than in 23-24 Hr *sev-GAL4>UAS-Ras1^{V12}* pupae (Fig. 2G-I). The salivary glands (SG), which normally disappear by this stage of pupal development, also persisted in pupae co-expressing *sev-GAL4>UAS-Ras1^{V12}* and *hsrω-RNAi* or *EP3037* beyond the 15-16 Hr APF stage (Fig. 2J-L). It may be noted that neither *sev-GAL4* nor *GMR-GAL4* expresses in SG or MT (Ray and Lakhotia 2015). The other early pupal phenotype persisting in the early dying pupae was the *sev-GAL4>UAS-GFP* expression in the 7 pairs of dorso-medial neurons in each of the posterior neuromeres in abdominal ganglia (Ray and Lakhotia, 2015). In *sev-GAL4>UAS-Ras1^{V12}* pupae (Fig. 2M), like that in wild type, all the 7 pairs of these dorso-medial neurons showed *UAS-GFP* expression at 8-9 Hr APF. As reported earlier (Ray and Lakhotia, 2015), the GFP expression in all of these, except the anterior-most pair, disappeared in 23-24 Hr old wild type and *sev-GAL4>UAS-Ras1^{V12}* pupae (Fig. 2P). However, all these 7 neuron pairs continued showing *UAS-GFP* expression in 23-24 Hr old *sev-GAL4>UAS-Ras1^{V12} hsrω-RNAi* or *sev-GAL4>UAS-Ras1^{V12} EP3037* pupae (Fig. 2Q, R). The small proportion of pupae of these genotypes that survived beyond 23-24 Hr APF showed normal developmental changes as in wild type or *sev-GAL4>UAS-Ras1^{V12}* pupae of comparable age. However, their later development was affected leading to late pupal death.

Unlike the 13-14 or 19-20 Hr old wild type pupae (Fig. 1M, Q), *GMR-GAL4>UAS-Ras1^{V12}* expressing pupae did not show demarcation of head, thorax and abdominal regions (Fig. 1N and R). A necrotic patch appeared by 19-20 Hr APF at prospective adult eye sites (Fig. 1R). The early disappearing dorso-medial pairs of neurons in the abdominal ganglia also continued to show GFP expression till 20-24 Hr APF (see Fig. 3I-L). Co-expression of *EP3037* or *hsrω-RNAi* with *GMR-GAL4>UAS-Ras1^{V12}* did not alter the time of pupal death (Fig. 1N-P, R-T).

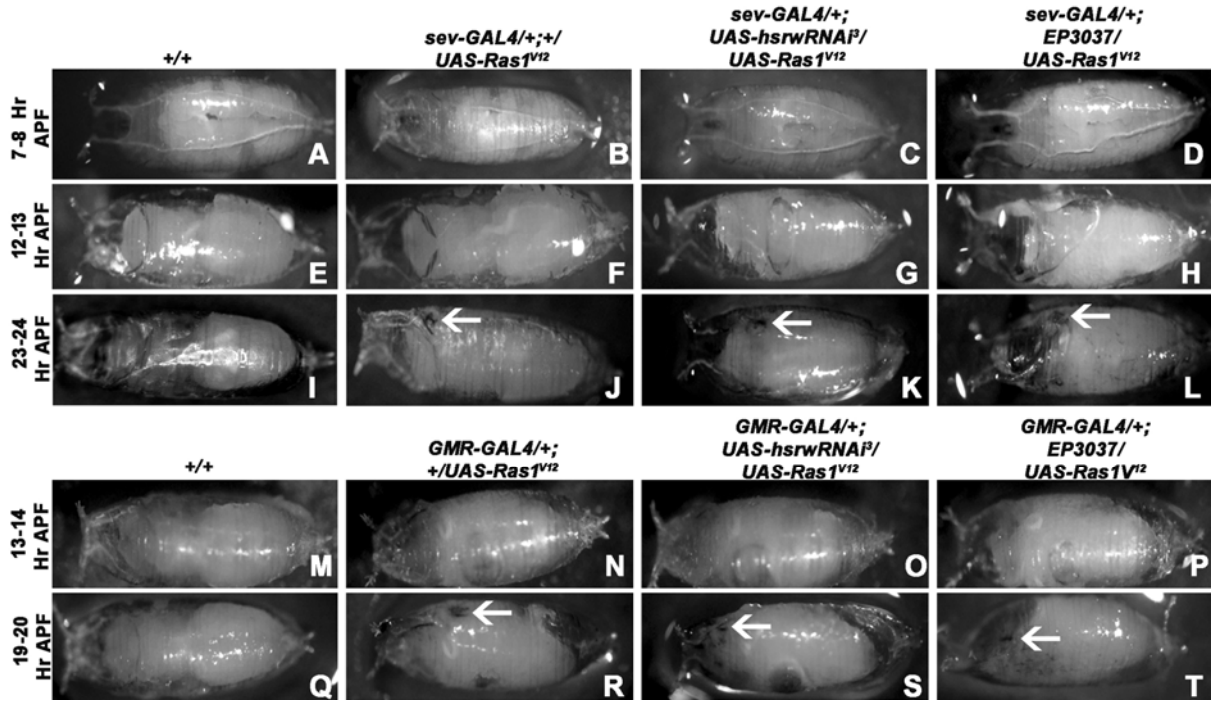

Fig. 1. ***sev-GAL4>UAS-Ras1^{V12} hsrω-RNAi*** **or** ***sev-GAL4>UAS-Ras1^{V12} EP3037*** **or** ***GMR-GAL4>UAS-Ras1^{V12}*** **show early pupal lethality accompanied by absence of prepupal to pupal metamorphic changes.** (**A-T**) Photomicrographs of pupae at different stages of development (noted on left of each row) in different genotypes (noted on top of the columns). White arrows in **J**-**L** and **R**-**T** indicate the necrotic patch near eye region.

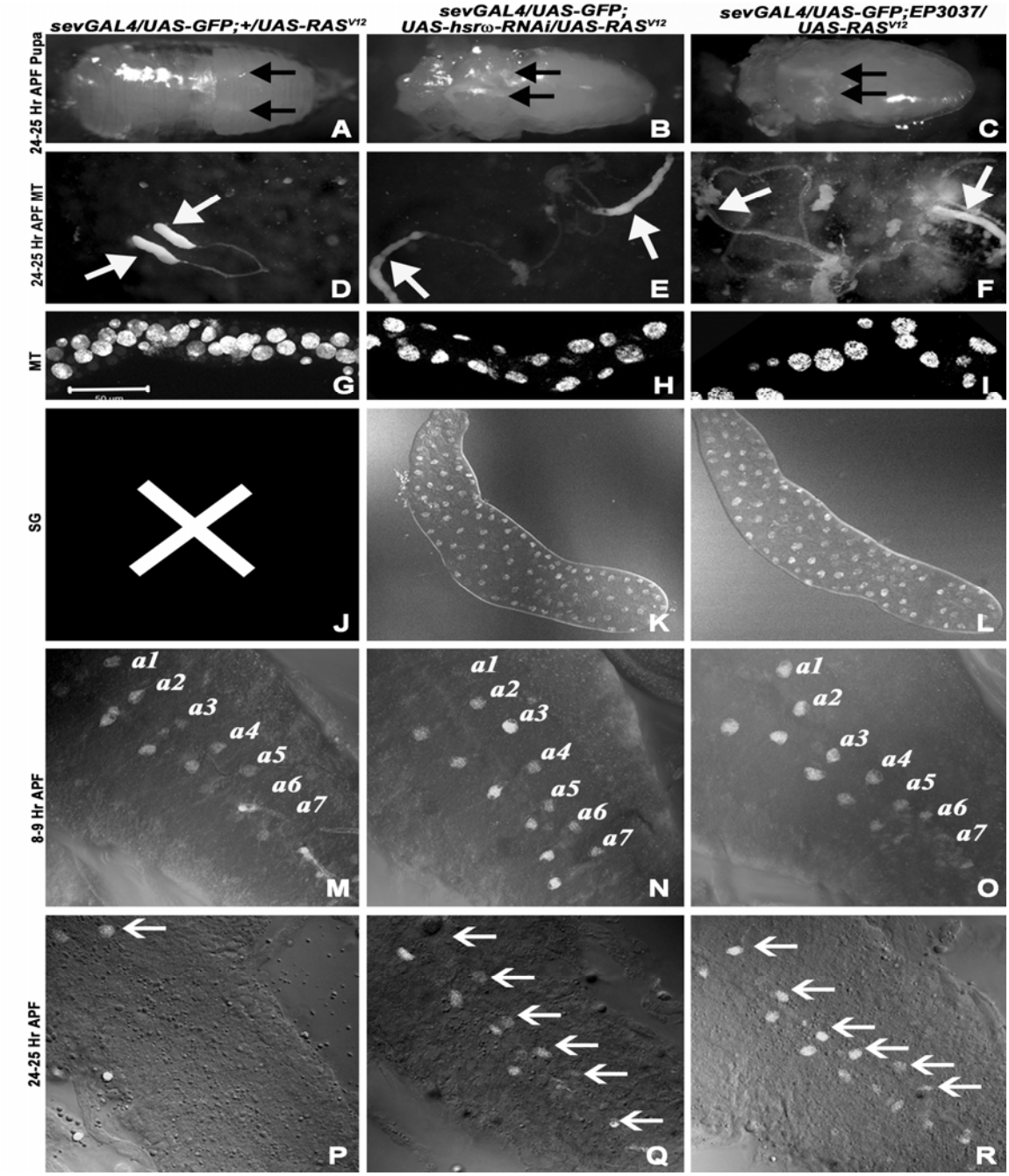

Fig. 2. The prepupal to pupal metamorphic changes in internal organs are affected in early dying pupae. (**A-C**) 24-25 Hr old pupae and (**D-F**) dissected out anterior MT of genotypes noted above each column. White arrows in **D-F** indicate the distal segments of anterior MT. (**G-L**) Confocal optical sections of DAPI stained MT (**G-I**) and SG (**J-L**) of 24-25 Hr pupae; a cross is marked at **J** as SG are no longer seen at 24-25 Hr APF in *sev-GAL4>UAS-Ras1*^{V12}. (**M-R**) Confocal projections of ventral ganglia showing *sev-GAL4*>UAS-GFP expressing (white) dorso-medial segmental paired neurons in abdominal segments (**a1** to **a7**, arrows) at 8-9 Hr APF (**M-O**) and at 24-25 Hr APF (**P-R**) stages in different genotypes noted above each column. Scale bar in **G** is 50µm and applies to **G-R**.

Ecdysone signaling at early pupal stages was compromised in the early dying pupae

Since the pupae dying around 25-30 Hr APF failed to undergo the early pupal changes that follow the ecdysone pulse beginning at 8-10 Hr APF (Handler, 1982), we examined the distribution of Broad, one of the early ecdysone signaling responders (Zhou et al., 2009; Zollman et al., 1994), in late third instar larval and pupal (12-13 and 24-25 Hr APF stage) ventral ganglia of different genotypes using a Broad-core antibody (Emery et al., 1994). Intense and uniform nuclear fluorescence with little cytoplasmic signal (Fig. 3A-D) was seen in Broad positive ventral ganglia cells from early pupal stages in all the genotypes (12-13 Hr APF). However, beginning at 16 Hr APF, distribution of Broad in *sev-GAL4>UAS-GFP* and *sev-GAL4>UAS-Ras1^{V12}* ventral ganglia changed from the uniform nuclear distribution, to a few intense peri-nuclear granules (Fig. 3E and F) with stronger cytoplasmic presence than in earlier stages. Ventral ganglia in pupae co-expressing *sev-GAL4* driven *hsrω-RNAi* or *EP3037* with *Ras1^{V12}* did not show these changes since at 24-25 Hr APF, most Broad positive cells continued show near uniform pan-nuclear distribution with low cytoplasmic presence (Fig. 3G, H). Although a few nuclei in the 24-25 Hr old pupal ventral ganglia co-expressing *sev-GAL4>Ras1^{V12}* and *hsrω-RNAi* or *EP3037* showed Broad in a punctate or granular form , these remained across the nuclear area rather than being typically peri-nuclear as in the same age *sev-GAL4>UAS-GFP* and *sev-GAL4>UAS-Ras1^{V12}* ventral ganglia (Fig. 3).

The *GMR-GAL4>UAS-GFP* expressing ventral ganglia from 16-17 and 20-21 Hr old pupae (Fig. 3I, K) showed the Broad protein as in corresponding age *sev-GAL4>UAS-GFP* and *sev-GAL4>UAS-Ras1^{V12}* pupae. However, the Broad protein retained its uniformly strong pan-nuclear distribution and low cytoplasmic presence in most of the Broad positive cells in *GMR-GAL4>UAS-Ras1^{V12}* ventral ganglia from 16-17 and 20-21 Hr old pupae (Fig. 3J, L).

Interestingly, none of the *sev-GAL4>UAS-GFP* or *GMR-GAL4>UAS-GFP* expressing neurons in the ventral ganglia (marked by white arrows in Fig 2E-H), showed Broad expression, neither at 8-9 Hr nor at 24-25 Hr APF stage (Fig. 3) in any of the genotypes.

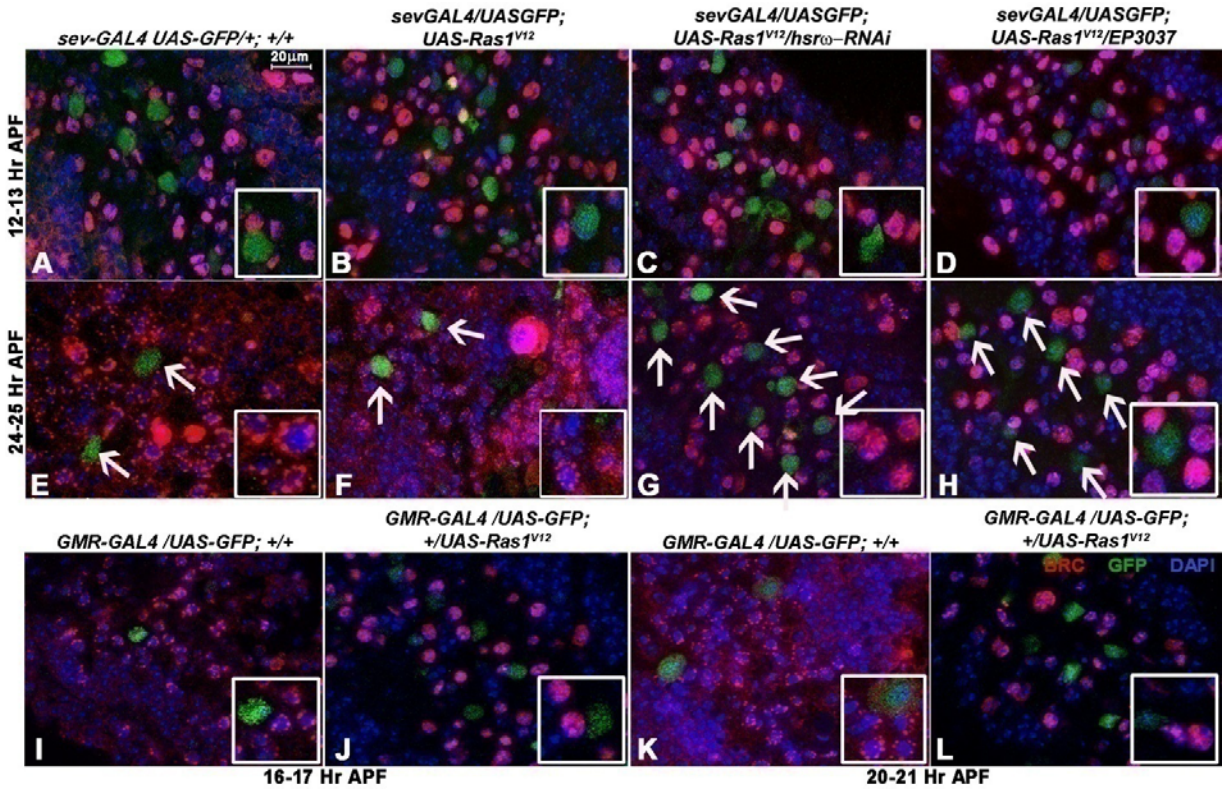

Fig. 3. Distribution of Broad protein in ventral ganglia cells at 16-17 Hr or later APF is affected in early dying pupae. (**A-H**) Confocal optical sections showing parts of ventral ganglia from 12-13 Hr (**A-D**) and 24-25 Hr (**E-H**) old pupae of different genotypes (noted above each column) immunostained with anti-Broad-core (red) and counterstained with DAPI (blue); GFP (green) marks the *sev-GAL4* expressing neurons (white arows). **(I-L)** Confocal optical sections of parts of ventral ganglia from 16-17 Hr (**I, J**) and 20-21 Hr (**K, L**) old pupae (genotypes noted above each image) immunostained with anti-Broad-core (red) and counterstained and with DAPI (blue); GFP (green) marks the *GMR-GAL4* expressing neurons. Inset in each panel shows higher magnification images of a few Broad expressing cells. Scale bar in (**A**) indicates 20µm and applies to all images.

The post-pupation ecdysone levels were reduced in early dying pupae

Above results indicated a failure of the post-pupation ecdysone signaling in pupae that would die 25-30 Hr APF. Immunoassay for 20-hydroxy-ecdysone indeed revealed ecdysone levels in 8-9 Hr old pupae expressing *sev-GAL4>UAS-Ras1*^{V12} alone or together with *hsrω-RNAi* transgene or *EP3037* allele to be comparable to those in similar age *sev-GAL4>UAS-GFP* pupae (Fig. 4A). However, 24-25 Hr old pupae co-expressing *hsrω-RNAi* or *EP3037* with *sev-GAL4>UAS-Ras1*^{V12} did not display the characteristic increase in ecdysone levels (Handler, 1982) seen in *sev-GAL4>UAS-GFP* or *sev-GAL4>UAS-Ras1*^{V12} or only the *sev-GAL4>hsrω-RNAi* transgene or *EP3037* (Fig. 4A). The ecdysone levels in *GMR-GAL4>UAS-Ras1*^{V12} 24-25 Hr APF stage pupae were also significantly lower than in the corresponding age *GMR-GAL4>UAS-GFP* control pupae (Fig 4B).

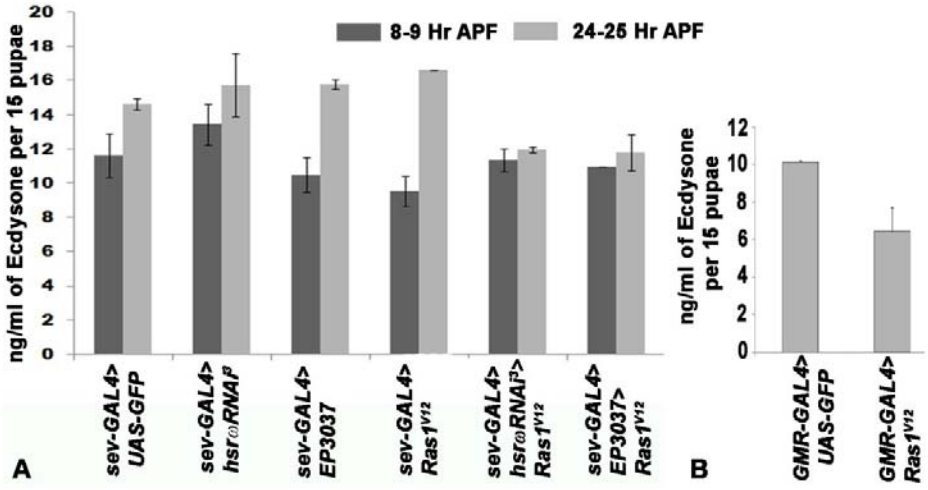

Fig. 4. **The expected increase in ecdysone levels in post 8-9 Hr pupae does not occur in pupae that are destined to die early. A-B** Bars showing mean (±S.E. of two independent replicates) levels of 20 hydroxy-ecdysone (Y axis) in different genotypes (X-axis) at 8-9 Hr APF (dark grey) and at 24-25 Hr APF stages (light grey). Each genotype also carries *UAS-GFP* transgene. The mean values in *sev-GAL4>UAS-Ras1^{V12} hsrω-RNAi* and *sev-GAL4>UAS-Ras1^{V12} EP3037* are significantly different (P<,0.05) from that in *sev-GAL4>UAS-Ras1^{V12}* samples.

Further support for reduced levels of ecdysone being responsible for the early pupal death was obtained by examining phenotypes of otherwise wild type early pupae in which the ecdysone levels were conditionally reduced using the temperature sensitive *ecd^{1}* allele (Henrich et al., 1987b). This temperature-sensitive mutation inhibits production of ecdysone when grown at the 29-30°C. The *sev-GAL4>UAS-GFP; ecd^{1}* larvae were reared at 24°C and 0-1 Hr old white prepupae were transferred to 30°C to conditionally inhibit ecdysone synthesis. About 50% of these pupae showed early death by 25-30 Hr APF while the remaining died as late pupae (Table 1). The *sev-GAL4>UAS-GFP; ecd^{1}* pupae, reared since beginning of pupation at 30°C, and dying at 24-25 Hr APF showed persistence of the dorso-medial pairs of segmental neurons in ventral ganglia, less compact arrangement of MT cells (Supplementary Fig. S1A, B) and other developmental defects seen in *sev-GAL4>UAS-Ras1^{V12} hsrω-RNAi* or *sev-GAL4>UAS-Ras1^{V12} EP3037*.

Externally provided ecdysone partially rescued the early pupal death

We exposed 8-9 Hr old pupae of different genotypes to exogenous ecdysone by incubating them in 1 µg/ml 20-hydroxyecdysone solution for 12 Hr, following which they were taken out, blotted dry and allowed to develop further in normal air. To confirm effectiveness of such exogenous exposure to ecdysone, we used *ecd^{1}* pupae as control. Fresh 0-1 Hr old *sev-GAL4>UAS-GFP; ecd^{1}* white prepupae, grown through the larval period at 24°C, were transferred to 30°C to block further ecdysone synthesis. After 8 Hr at 30°C, they were transferred to the 20-hydroxy-ecdysone solution for 12 Hr at 30°C to keep the endogenous ecdysone synthesis inhibited, while it was provided in the incubation medium. After the 12 Hr ecdysone exposure, the pupae were

returned to 30°C for further development. As seen from the data in Table 1, about 50% *sev-GAL4>UAS-GFP; ecd*^{1} pupae maintained at 30°C from 0-1 Hr pre-pupa stage onwards without any exogenous ecdysone died by 25-30 Hr APF. However, there was a 2-fold reduction in the early dying *ecd*^{1} pupae maintained at 30°C but exposed to exogenous ecdysone from 8 to 20 Hr APF (Table 1). None, however eclosed. Significantly, the pre-pupal to pupal metamorphic changes in these surviving pupae occurred normally so that the dorso-medial pairs of segmental neurons in ventral ganglia and MT displayed the expected changes (Supplementary Fig. S1C, D). Survival of a significant proportion of *ecd*^{1} pupae, maintained at 30°C while being exposed to exogenous ecdysone, clearly indicated that the moulting hormone penetrated the early pupal case in at least some of them. The failure of all pupae exposed to exogenous ecdysone to survive beyond the early stage may indicate a variable penetration through pupal case.

When 8-9 Hr old pupae co-expressing *sev-GAL4>UAS-Ras1*^{V12} *hsrω-RNAi* or *sev-GAL4>UAS-Ras1*^{V12} *EP3037* were exposed to exogenous 20-hydroxy-ecdysone as above, there was a near 2-fold increase in those continuing to develop to late stages, although none of them emerged as flies (Table 1). The somewhat lesser increase (1.4 fold, Table 1) in survival of the ecdysone exposed *sev-GAL4>UAS-Ras1*^{V12} *hsrω-RNAi* pupae beyond the early stage may be related to the fact that a larger proportion of them die early (see above, Fig. 1).

Together, these results confirm that *sev-GAL4>UAS-Ras1*^{V12} *hsrω-RNAi* and *sev-GAL4>UAS-Ras1*^{V12} *EP3037* or *GMR-GAL4>UAS-Ras1*^{V12} fail to release ecdysone after the 8-9 Hr pupal stage and therefore, do not undergo the expected metamorphic changes.

Table 1. Exogenous ecdysone partially suppressed early pupal death in *sev-GAL4>UAS-GFP; ecd*^{1} (maintained at restrictive temperature from 0 Hr pre-pupa onwards), *sev-GAL4>UAS-Ras1*^{V12} *hsrω-RNAi* and *sev-GAL4>UAS-Ras1*^{V12} *EP3037* pupae

Treatment	**Genotype**								
	***sev-GAL4>UAS-GFP; ecd*^{1} at 30^{0}C**			***sev-GAL4>UAS-Ras1*^{V12} *hsrω-RNAi* at 24^{0}C**			***sev-GAL4>UAS-Ras1*^{V12} *EP3037* at 24^{0}C**		
	N	**Early Pupal Death**	**Late Pupal Death**	**N**	**Early Pupal Death**	**Late Pupal Death**	**N**	**Early Pupal Death**	**Late Pupal Death**
a. Control	**43**	**54%**	**46%**	**49**	**82%**	**18%**	**38**	**71%**	**29%**
b. Ecdysone treatment*	**48**	**27%**	**73%**	**62**	**58%**	**42%**	**50**	**32%**	**68%**
Fold change in time of death (a/b)		**2 Fold decrease**			**1.4 Fold decrease**			**2.2 Fold decrease**	

* 8 Hr old pupae incubated in ecdysone (1µg/ml) containing PBS for 12 Hr at the indicated temperature following which they were blotted dry and monitored for their subsequent development.

N = total number of pupae examined

Early dying pupae had lowered *ptth* and Halloween gene transcripts but elevated expression of *dilp8* and some JNK pathway genes

Since the *GMR-GAL4* and *sev-GAL4* drivers do not express in prothoracic gland (Ray and Lakhotia, 2015), the site of ecdysone production, a reduction in ecdysone levels in early pupae indicated some inter-tissue signaling. To identify the signals, total RNAs from 16-17 Hr old pupae of different genotypes (*sev-GAL4>UAS-GFP, sev-GAL4>UAS-Ras1^{V12}*, *sev-GAL4>UAS-Ras1^{V12} hsrω-RNAi* and *sev-GAL4>UAS-Ras1^{V12} EP3037*) were used for a microarray based transcriptome analysis. A pair wise comparison between different genotypes revealed significant up- or down-regulation of many genes belonging to diverse GO categories (Supplementary Table S1). In order to narrow down on genes which may be causally associated with the early pupal death, we focused on those that were commonly up- or down-regulated in *sev-GAL4>UAS-Ras1^{V12} hsrω-RNAi* and *sev-GAL4>UAS-Ras1^{V12} EP3037* samples in comparison to *sev-GAL4>UAS-Ras1^{V12}* (columns 1 and 2 in Supplementary Table S1). The commonly up-regulated groups of genes in *sev-GAL4>UAS-Ras1^{V12} hsrω-RNAi* and *sev-GAL4>UAS-Ras1^{V12} EP3037* pupae included, among many others, those associated with stress responses, cell and tissue death pathways, autophagy, toll signaling, innate immune system etc. Some of these seem to be primarily due to activated Ras or altered *hsrω* expression since the Ras/MAPK pathway is known to regulate immune response (Hauling et al., 2014; Ragab et al., 2011) while the *hsrω* transcripts have roles in stress responses, cell death and several other pathways (Lakhotia, 2011; Lakhotia, 2016; Mallik and Lakhotia, 2009a)(Ray and Lakhotia, 2017). More interestingly, several genes involved in lipid and steroid biosynthesis processes were commonly down-regulated in both the genotypes showing early pupal death (*sev-GAL4>UAS-Ras1^{V12} hsrω-RNAi* and *sev-GAL4>UAS-Ras1^{V12} EP3037*; see Supplementary Table S1).

Since damaged or tumorous imaginal discs are reported (Colombani et al., 2012; Garelli et al., 2012) to affect ecdysone synthesis through up regulation of JNK signaling and Dilp8 secretion, we examined the microarray data for levels of transcripts of genes involved in ecdysone biosynthesis and insulin- and JNK-signaling pathways through pair wise comparisons of different genotypes (Supplementary Table S2), taking >1.5 fold difference as significant. Three (*spookier, phantom* and *shadow*) of the five 20-hydroxy-ecdysone synthesis related Halloween genes (Huang et al., 2008) showed consistent down-regulation in *sev-GAL4>UAS-Ras1^{V12} hsrω-RNAi* and *sev-GAL4>UAS-Ras1^{V12} EP3037* when compared with *sev-GAL4>UAS-Ras1^{V12}* pupae, while *shade* did not change and *disembodied* displayed up-regulation. Down-regulation of spookier, phantom and shadow transcripts in 16-17 Hr old *sev-GAL4>UAS-Ras1^{V12} hsrω-RNAi* and *sev-GAL4>UAS-Ras1^{V12} EP3037* pupae correlates with the above noted (Fig. 4) reduced ecdysone levels since while the *spookier* and *phantom* genes act at early stages in ecdysone biosynthesis (Huang et al., 2008), the *shadow* gene product converts 2-deoxyecdysone into ecdysone (Warren et al., 2002).

Of the eight known Dilps (Dilp1-8) in *Drosophila* (Nässel et al., 2013), only *dilp8* showed significant up-regulation in *sev-GAL4>UAS-Ras1^{V12} hsrω-RNAi* and *sev-GAL4>UAS-Ras1^{V12}*

EP3037 genotypes when compared with *sev-GAL4>UAS-GFP* or *sev-GAL4>UAS-Ras1^{V12}* (Supplementary Table S2). Interestingly, the *dilp8* transcripts in *sev-GAL4>UAS-Ras1^{V12} hsrω-RNAi* showed about 2 fold greater increase than in *sev-GAL4>UAS-Ras1^{V12} EP3037*, which correlates with the much higher frequency of death as in the former case (Table 1).

Like the *dilp8*, transcripts of *tobi* (*target of brain insulin*) were also significantly up-regulated (Supplementary Table S2) when *sev-GAL4>UAS-Ras1^{V12}* was co-expressed with *hsrω-RNAi* or *EP3037*. The Dilp8 action on ecdysone synthesis in prothoracic gland is reported to involve the neuronal relaxin receptor Lgr3 (Colombani et al., 2015; Garelli et al., 2015). Our microarray data indicated that the *lgr3* transcripts were only marginally elevated in *sev-GAL4>UAS-Ras1^{V12} hsrω-RNAi* expressing early pupae but not significantly affected in *sev-GAL4>UAS-Ras1^{V12} EP3037* individuals.

Analysis of the microarray data for total RNA from 16-17 Hr old pupae revealed considerable variability in levels of different JNK-signaling pathway members in different genotypes (Supplementary Table S2). Interestingly, a greater number of the JNK pathway genes were up-regulated in *sev-GAL4>UAS-Ras1^{V12} hsrω-RNAi* than in *sev-GAL4>UAS-GFP* or *sev-GAL4>UAS-Ras1^{V12}* genotypes. On the other hand, some of the JNK pathway genes appeared down-regulated in *sev-GAL4>UAS-Ras1^{V12} EP3037* genotypes than in *sev-GAL4>UAS-GFP* or *sev-GAL4>UAS-Ras1^{V12}* (Supplementary Table S2). However, genes like *eiger*, *gadd45* and *takl1* (*tak1-like 1*) were significantly up-regulated in *sev-GAL4>UAS-Ras1^{V12} hsrω-RNAi* and in *sev-GAL4>UAS-Ras1^{V12} EP3037* genotypes, while *tak1* was down-regulated in both. Notably, the fold change for each of these genes was greater in case of *sev-GAL4>UAS-Ras1^{V12} hsrω-RNAi* than in *sev-GAL4>UAS-Ras1^{V12}* EP3037.

We validated some of the microarray data by qRT-PCR using RNA samples from late larval and early pupal (8-9 Hr APF) eye discs and/or prothoracic glands (Fig. 5A). In agreement with the microarray data for whole pupal RNA, qRT-PCR of 8-9 Hr old pupal eye disc RNA confirmed significant up-regulation of transcripts of the JNK signaling pathway genes like *tak1-like 1, eiger 2, gadd45* and *puckered* in *sev-GAL4>UAS-Ras1^{V12} hsrω-RNAi* and *sev-GAL4>UAS-Ras1^{V12} EP3037* when compared with same age *sev-GAL4>UAS-Ras1^{V12}* eye discs (Fig. 5A). Interestingly late third instar larval eye discs of different genotypes did not show much difference for these transcripts (Fig. 5A).

Quantification of *dilp8* transcripts from late third instar larval and 8-9 Hr pupal eye discs of different genotypes by qRT-PCR revealed, in agreement with microarray data for total pupal RNA, substantial increase (65-120 folds) in *dilp8* transcripts in *sev-GAL4>UAS-Ras1^{V12} hsrω-RNAi* and *sev-GAL4>UAS-Ras1^{V12} EP3037* pupal eye discs when compared with those expressing only the activated Ras (Fig. 5A). However, *dilp8* transcript levels in late third instar larval eye discs showed only a marginal up-regulation in *sev-GAL4>UAS-Ras1^{V12} hsrω-RNAi* and *sev-GAL4>UAS-Ras1^{V12} EP3037* eye discs (Fig. 5A). Compared to *sev-GAL4>UAS-Ras1^{V12}*, the brain lobes and ventral ganglia of early dying pupae also showed increase in *dilp8* transcripts, more so in brain lobes of *sev-GAL4>UAS-Ras1^{V12} hsrω-RNAi* (Fig. 5B).

Down-regulation of *spookier* and *phantom* transcripts in *sev-GAL4>UAS-Ras1^{V12} hsrω-RNAi* and *sev-GAL4>UAS-Ras1^{V12} EP3037* genotypes was validated by qRT-PCR using 8-9 Hr old pupal prothoracic gland RNA. Compared to *sev-GAL4>UAS-Ras1^{V12}*, both transcripts showed greater reduction in *sev-GAL4>UAS-Ras1^{V12} hsrω-RNAi* and *sev-GAL4>UAS-Ras1^{V12} EP3037* pupal (Fig 5A) than in larval prothoracic glands. Intriguingly, *sev-GAL4>UAS-Ras1^{V12} hsrω-RNAi* larval prothoracic glands showed up-regulation of *spookier* and *phantom* transcripts (Fig. 5A).

Since Dilp8 reportedly inhibits ecdysone synthesis triggering signals via the brain (Colombani et al., 2012; Garelli et al., 2012), we examined levels of *ptth* transcripts in brain in the early dying pupae. We also checked the transcripts of Dilp8 receptor in brain (Colombani et al., 2015; Vallejo et al., 2015). The *ptth* transcripts were less abundant in larval brain lobes of early dying individuals, and further reduced in early pupae so that no transcripts were detected in pupal brain lobes of *sev-GAL4>UAS-Ras1^{V12} hsrω-RNAi* (Fig 5B). On the other hand, transcripts of none of the three Dilp8 receptors, viz., *lgr3*, *inr* and *drl*, showed any substantial change in early pupal ventral ganglia although these transcripts were reduced in brain lobes. Surprisingly, compared to *sev-GAL4>UAS-Ras1^{V12}*, the *inr* transcripts showed about 4 fold up-regulation in *sev-GAL4>UAS-Ras1^{V12} EP3037* (Fig 5B). Since there was no change in *dilp8* transcripts in eye discs of third instar larvae, levels of the Dilp8 receptor transcripts were not examined in larval brain lobes.

The *gadd45* transcripts showed only a two fold increase in 8-9 Hr old pupal brain lobes and ventral ganglia (Fig 5B) from genotypes that die as early pupae.

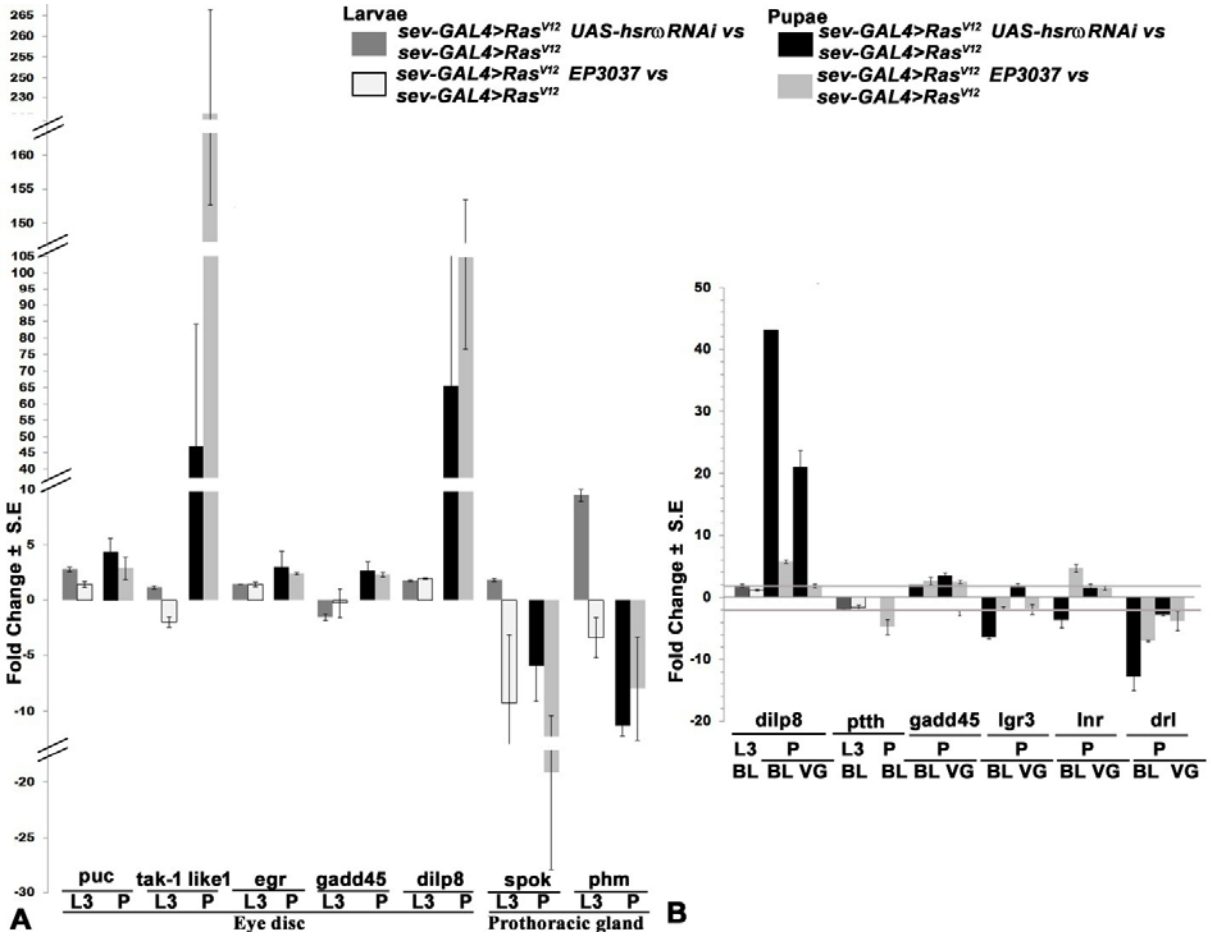

Fig. 5. Transcript levels of some JNK pathway, *dilp8*, *ptth* and ecdysone biosynthesis pathway genes are significantly changed at early pupal but not late larval stages in genotypes showing early pupal death. A Histograms showing qRT-PCR based mean fold changes (±S.E., Y-axis) in different transcripts in eye discs or prothoracic glands (X-axis) of *sev-GAL4>UAS-Ras1^{V12} hsrω-RNAi* and *sev-GAL4>UAS-Ras1^{V12} EP3037* late 3rd instar larvae (L3) or 8-9 Hr old pupae (P) when compared with *sev-GAL4>UAS-Ras1^{V12}*. **B** Histograms showing qRT-PCR based mean (±S.E.) fold changes (Y-axis) in different transcripts (X-axis) in brain lobes (BL) or ventral ganglia (VG) of *sev-GAL4>UAS-Ras1^{V12} hsrω-RNAi* and *sev-GAL4>UAS-Ras1^{V12} EP3037* late 3rd instar larvae (L3) or 8-9 Hr old pupae (P) when compared with *sev-GAL4>UAS-Ras1^{V12}*. Grey lines mark the plus and minus two fold change compared to the controls. Keys for different bars are provided at top.

Dilp8 protein levels elevated in early pupal eye discs but not in larval eye discs or in larval and pupal CNS in early dying genotypes

Immunostaining of eye discs with Dilp8 antibody (Colombani et al., 2012) revealed absence of Dilp8 staining in the ommatidial cells (Fig. 6A-D) but a faint presence of Dilp8 in the cytoplasm of peripodial cells of late third instar larval eye discs of all the genotypes (Fig. 6I-L). The Dilp8

staining in ommatidial cells of 8-9 Hr pupal eye discs co-expressing *sev-GAL4>UAS-Ras1^{V12}* and *hsrω-RNAi* or *sev-GAL4>UAS-Ras1^{V12} EP3037* was also faint (Fig. 6E-H) but that in peripodial cells (Fig. 6M-P) was strong (Fig. 6O-P) compared with that in *sev-GAL4>UAS-GFP* (Fig. 6M) or *sev-GAL4>UAS-Ras1^{V12}* (Fig. 6N) (for quantification of immunostaining, see Supplementary Fig. S2).

Since the *sevGAL4* and *GMR-GAL4* drivers also express in certain neurons in brain lobes and ventral ganglia (Ray and Lakhotia, 2015), we immunostained early pupal CNS of 8-9 Hr old pupae in *sevGL4>UAS-GFP*, *sev-GAL4>UAS-Ras1^{V12}*, *sev-GAL4>UAS-Ras1^{V12} hsrω-RNAi* and *sev-GAL4>UAS-Ras1^{V12} EP3037* (Fig. 7A-H). A low abundance of Dilp8 was seen all through the brain and ventral ganglia of *sevGL4>UAS-GFP* (Fig. 7A, E, I). Interestingly, none of the *sevGAL4>UAS-GFP* and *Ras^{V12}* transgene expressing neurons in brain and ventral ganglia (Ray and Lakhotia, 2015) of *sev-GAL4>UAS-Ras1^{V12}*, showed elevation in Dilp8 expression beyond the low expression seen in adjoining cells (Fig. 7J). Likewise, the Dilp8 expression in the 8-9 Hr old pupal *sev-GAL4>UAS-Ras1^{V12} hsrω-RNAi* and *sev-GAL4>UAS-Ras1^{V12} EP3037* brain lobes and ventral ganglia remained similar to that in *sevGAL4>UAS-GFP* and *sev-GAL4>UAS-Ras1^{V12}* (Fig. 7A-L). Intriguingly, a group of 4 neurons in mid-lateral part in each of the brain-hemispheres in all the four genotypes showed strong Dilp8 presence in cytoplasm and their axonal projections, which followed a semi-circular path to reach posterior part of the prothoracic gland (Fig. 7E-H). The posterior part of prothoracic gland also showed strong Dilp8 staining. However, unlike the above noted increase in *dilp8* transcripts in early pupal CNS of *sev-GAL4>UAS-Ras1^{V12} hsrω-RNAi* and *sev-GAL4>UAS-Ras1^{V12} EP3037*, levels of Dilp8 protein staining in CNS, including these specific 4 pairs of neurons and the basal part of the prothoracic gland, remained comparable in all the genotypes. Thus, despite the increase in *dilp8* transcripts, the *sevGAL4* driven expression of activated Ras without or with concurrent altered *hsrω* expression did not affect Dilp8 protein levels in the CNS.

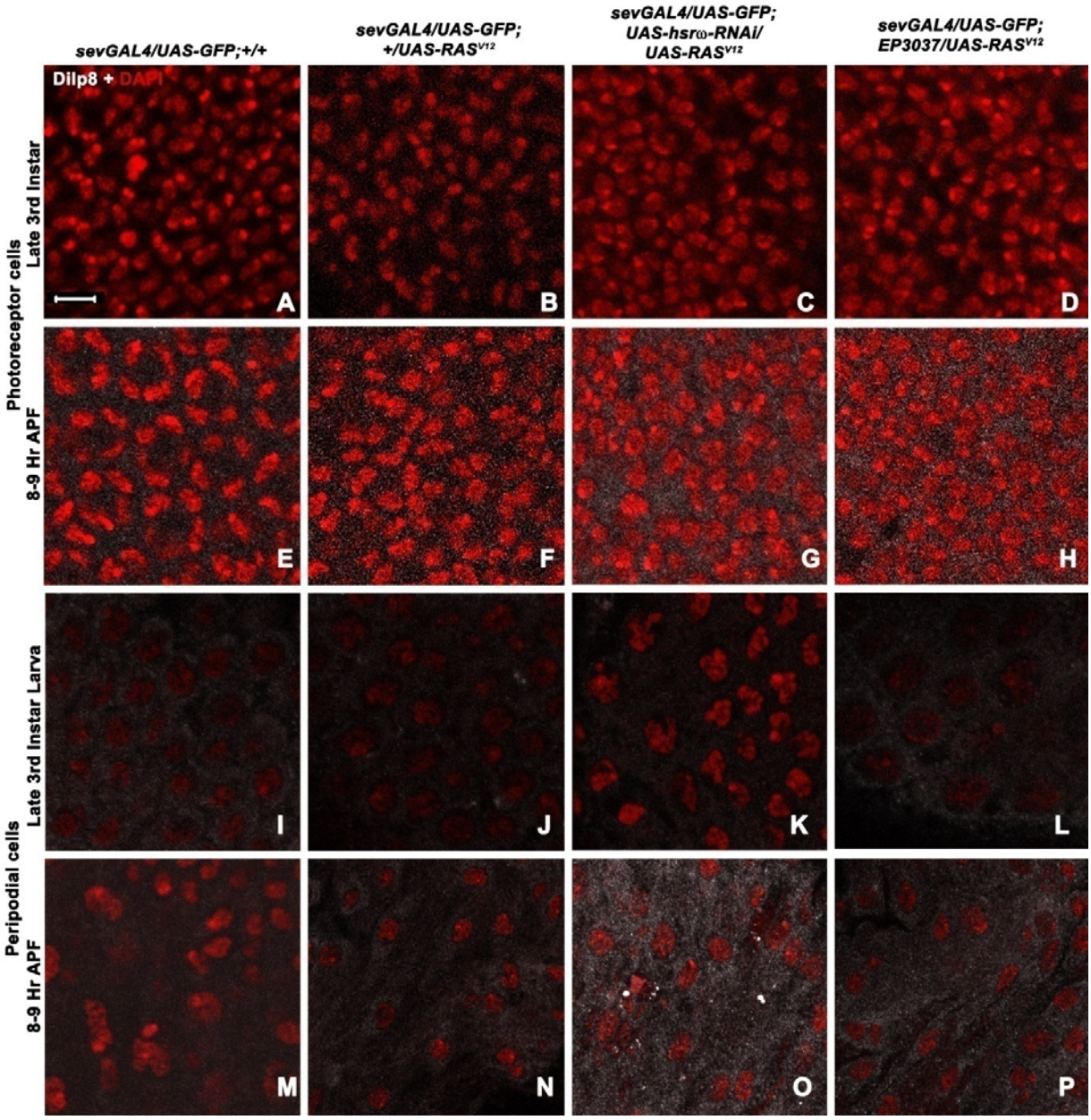

Fig 6. Expression of Dilp8 remains unchanged in eye discs of third instar larvae but increases in those of 8-9 Hr pupae in genotypes showing early pupal death. A-P Confocal optical sections of photoreceptor cells in third instar larval (**A-D**) and 8-9 Hr pupal eye discs (**E-H**), and peripodial cells in third instar (**I-L**) and 8-9 Hr pupa; eye discs (**M-P**) showing Dilp8 (white) in different genotypes (noted on top of each column). DAPI stained nuclei are in red. Scale bar in **A** denotes 5μm and applies to **A-P**

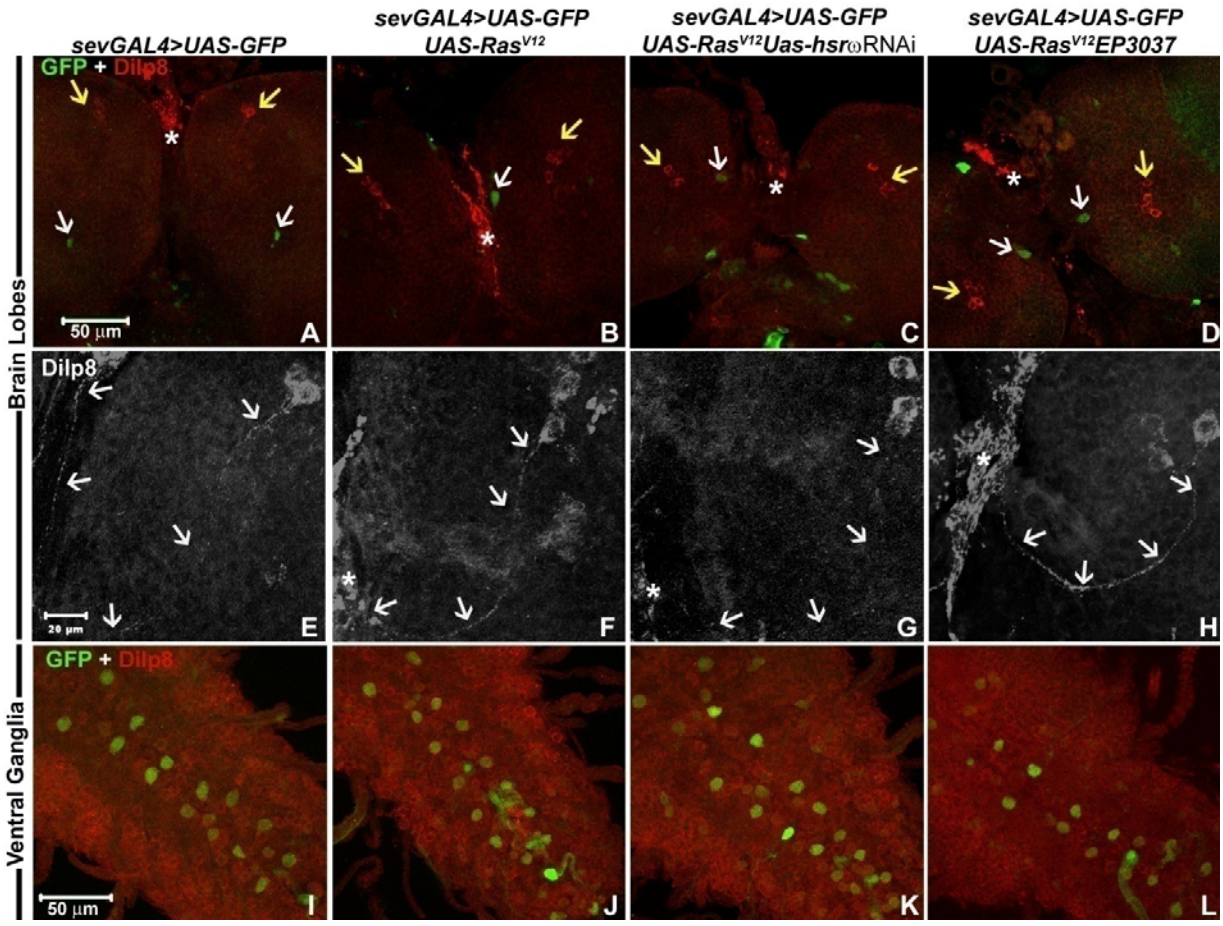

Fig. 7. Ectopic expression of activated Ras does not affect Dilp8 levels and distribution in brain lobes and ventral ganglia of 8-9 Hr old pupae. Confocal projection images of parts of brain lobes (**A**-**H**) and ventral ganglia (**I**-**L**) of 8-9 Hr old pupae of different genotypes (noted on top of each column) showing Dilp8 (red in **A**-**D** and **I**-**L**, white in **E**-**H**) and *sev-GAL4>GFP* (green in **A**-**D** and **I**-**L**). White arrows in **A**-**D** indicate the GFP-positive neurons in antero-medial part while the yellow arrows indicate the mid-lateral groups of four Dilp8 expressing neurons in each brain lobe; the basal region of prothoracic gland is marked with asterisk. **E**-**H** show higher magnification images of Dilp8 staining in one of the brain lobes with the white arrows indicating the Dilp8 positive axonal projections from the group of Dilp8 positive neurons to the basal region of prothoracic gland (marked by asterisk). The scale bar (50 µm) in **A** applies to **A**-**D** while that in **I** (20 µm) applies to **I**-**L**.

Phosphorylated JNK elevated in larval and pupal eye discs but not in CNS in early dying genotypes

Immunostaining for phosphorylated JNK (p-JNK, Basket) in *sev-GAL4>UAS-GFP* late third instar eye discs revealed low cytoplasmic p-JNK in photoreceptor cells (Fig. 8A). Photoreceptor cells from *sev-GAL4>UAS-Ras1^{V12}* larval discs showed slightly elevated p-JNK staining (Fig. 8B). Interestingly, co-expression of *hsrω-RNAi* transgene with *sev-GAL4>UAS-Ras1^{V12}* resulted

in a much greater increase in p-JNK (Fig. 8C) than when hsrω transcripts were up-regulated in *sev-GAL4>UAS-Ras1*^{V12} larval eye discs (Fig. 8D). Immunostaining for p-JNK in 8-9 Hr pupal eye discs also showed increase in *sev-GAL4>UAS-Ras1*^{V12} *hsrω-RNAi* and in *sev-GAL4>UAS-Ras1*^{V12} *EP3037* compared to *sev-GAL4>UAS-Ras1*^{V12} (Supplementary Fig. S3A-C). For quantification of the p-JNK immunostaining in larval eye discs of these different genotypes, we used the Histo tool of the LSM510 Meta software on projection images of 12 optical sections through the photoreceptor arrays in each genotype. The data are presented in Fig. 8M.

It is notable that the p-JNK staining increased not only in the *sev-GAL4* expressing cells in ommatidial units, but also in neighbouring non-GFP expressing cells and in the more distant peripodial cells of larval eye discs (Supplementary Fig. S4). This is in agreement with our earlier finding (Ray and Lakhotia, 2017, pre-print) of cell non-autonomous spread of activated Ras signaling in these genotypes.

Immunostaining of 8-9 Hr old pupal brain ganglia for p-JNK revealed that its expression was not affected by *sevGAL4>UAS-Ras*^{V12} expression, without or with concurrent altered *hsrω* levels. Brain lobes showed comparable JNK staining in all the genotypes with a stronger expression in the Mushroom body (Fig. 8E-H).

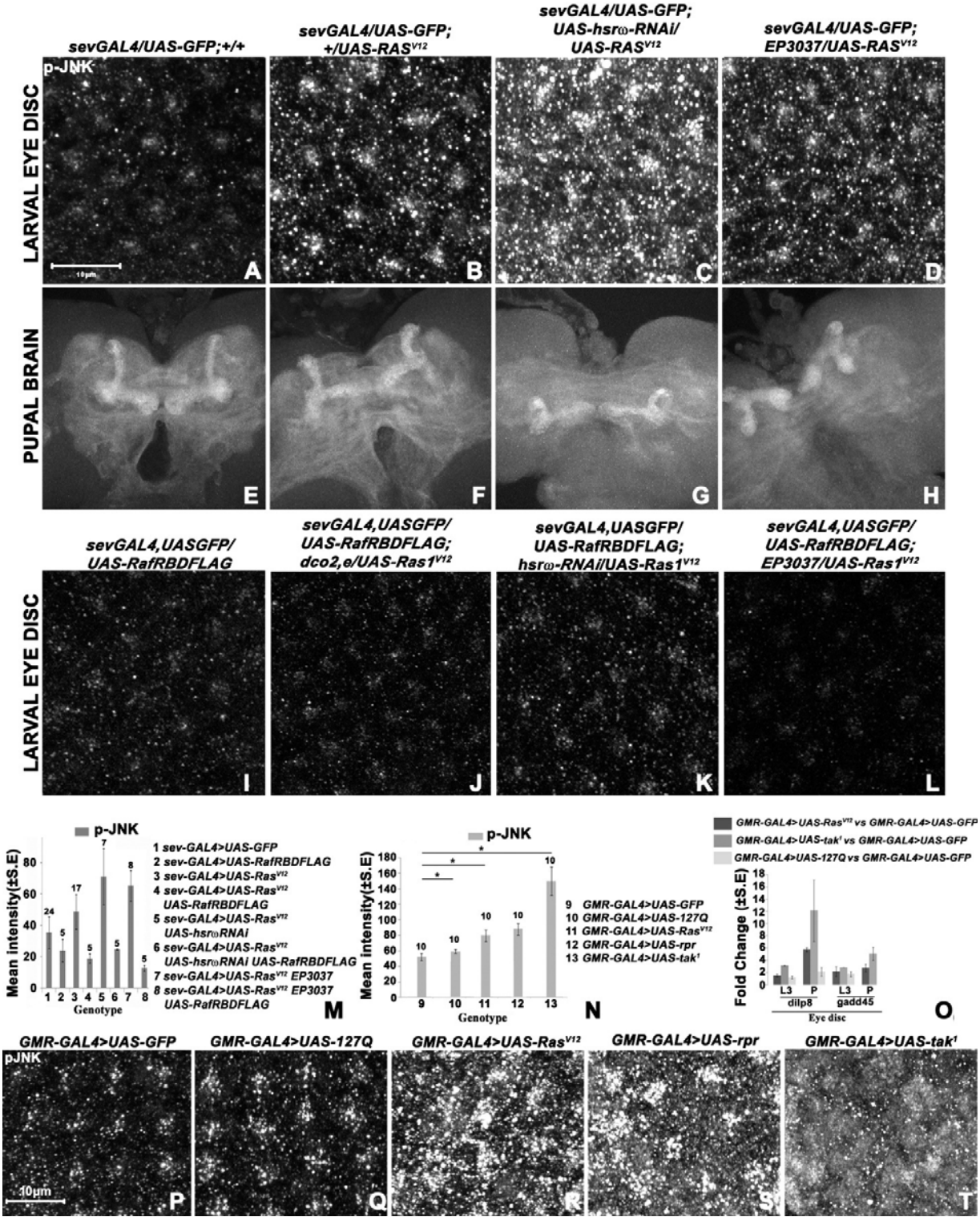

Fig. 8. **Expressions of phosphorylated JNK (p-JNK) and Dilp8 are enhanced in eye discs of early dying pupae. A-L** Confocal projection images of third instar larval eye discs (**A-D** and **I-L**) and 8-9 Hr pupal brain (**E-H**) showing p-JNK (white) in different genotypes (noted above the columns). Scale bar in

A denotes 10µm and applies to **A-L. M-N** Histograms showing mean (± S. E.) fluorescence intensity (Y-axis) of p-JNK in the eye discs of different genotypes (1-13, indexed on right side); number on top of each bar indicates the number of eye discs examined. **O** Histogram showing qRT-PCR based mean (±S.E. based on two biological replicates) fold changes (Y-axis) in levels of different transcripts (X-axis) in eye discs of *GMR-GAL4>UAS-Ras1^{V12}* (black bars), *GMR-GAL4>UAS-tak^{1}* (dark gray bars) and *GMR-GAL4>UAS-127Q* (light gray bars) late 3rd instar larvae (L3) or 8-9 Hr old pupae (P) when compared to control *GMR-GAL4>UAS-GFP*. **P-T** Confocal projection images of parts of third instar larval eye discs in genotypes mentioned on top of each panel showing distribution of p-JNK. Scale bar in **P** denotes 10µm and applies to **P-T.**

Reduction in Ras signaling in eye discs rescued early pupal lethality

We have recently reported (Ray and Lakhotia, 2017) that *sev-GAL4* driven co-expression of *Ras1^{V12}* with *hsrω-RNAi* or *EP3037* substantially enhances activated Ras levels in eye discs. To ascertain if the elevated Ras signaling dependent increase in p-JNK levels in eye discs co-expressing *sev-GAL4>Ras1^{V12}* with *hsrω-RNAi* or *EP3037* was indeed responsible for early pupal death we co-expressed *UAS-RafRBDFLAG* in these genotypes. The RafRBDFLAG acts as a dominant negative suppressor of Ras signaling (Freeman et al., 2010). Interestingly, there was no pupal lethality when *RafRBDFLAG* was co-expressed with *sev-GAL4>Ras1^{V12}* without or with *hsrω-RNAi* or *EP3037* expression (see Table 2). Concomitantly, the p-JNK levels were also not elevated in any of the genotypes when compared with those in *sev-GAL4>UAS-GFP/UAS-RafRBDFLAG* eye discs (Fig. 8I-L). As shown in Fig. 8M, the p-JNK level in *sev-GAL4>UAS-Ras1^{V12} hsrω-RNAi* and *sev-GAL4>UAS-Ras1^{V12} EP3037* eye discs co-expressing RafRBDFLAG remained low as in *sev-GAL4>UAS-GFP* control discs.

In order to further check that the *sev-GAL4>UAS-Ras1^{V12}* expression with co-altered *hsrω* transcript levels leads to pupal death through elevated JNK signaling and consequent high Dilp8 secretion, we co-expressed *UAS-bsk^{DN}*, a dominant negative suppressor of JNK signaling (Martín-Blanco et al., 1998), or *UAS-Dilp8RNAi* (Garelli et al., 2012) in *sev-GAL4>UAS-Ras1^{V12} hsrω-RNAi* and *sev-GAL4>UAS-Ras1^{V12} EP3037* eye discs. Contrary to expectation, neither of these rescued the early pupal lethality (data not presented). We believe that the ineffectiveness of *UAS-bsk^{DN}* or *UAS-Dilp8RNAi* co-expression in suppressing the early pupal lethality associated with *sev-GAL4>UAS-Ras1^{V12} hsrω-RNAi* and *sev-GAL4>UAS-Ras1^{V12} EP3037* is related to our earlier (Ray and Lakhotia, 2017) and present finding that the Ras signaling in these eye discs spreads non-autonomously to neighbouring as well as distant cells that themselves do not express *sev-GAL4*. Since the *sev-GAL4>UAS-bsk^{DN}* expression would remain limited to the few *sev-GAL4* expressing cells, it cannot suppress the high JNK signaling emanating from the other eye disc cells (Supplementary Fig. S4) following the cell non-autonomous spread of activated Ras. Likewise the *sev-GAL4>UAS-Dilp8RNAi* expression, limited to the few *sev-GAL4* expressing cells, would not suppress the JNK-triggered Dilp8 secretion by the peripodial cells.

GMR-GAL4 or _sev-GAL4_ or _MS1096-GAL4_ driven expression of enhanced JNK levels in eye or wing discs also result in early pupal death

We examined if other cases of early pupal lethality following expression of certain transgenes in imaginal discs are also associated with elevated JNK and Dilp8 signaling. We compared pupal lethality, and *dilp8* and/or pJNK levels in *UAS-GFP* or *UAS-Ras1^{V12}* with those in *GMR-GAL4>UAS-127Q* or *GMR-GAL4>UAS-rpr* or *GMR-GAL4>UAS-tak^{1}* eye discs. *GMR-GAL4* driven expression of *UAS-GFP* or *UAS-127Q* does not cause any pupal lethality (above results and (Mallik and Lakhotia, 2009b) while that of *UAS–rpr* (Table 2, also see (Morris et al., 2006) or *UAS-tak^{1}* (Table 2) caused early pupal death as in *GMR-GAL4>UAS-Ras1^{V12}* or *sev-GAL4>UAS-Ras1^{V12} UAS-hsrωRNAi* or *sev-GAL4>UAS-Ras1^{V12} EP3037*. Immunostaining for p-JNK in late larval eye discs of these different genotypes revealed that while those from *GMR-GAL4>UAS-GFP* or *GMR-GAL4>UAS-127Q* (Fig. 8P and Q) showed the normal low to moderate p-JNK, those expressing *GMR-GAL4>UAS-Ras1^{V12}* or *UAS–rpr* or *UAS-tak1* displayed very high p-JNK staining (Fig. 8N, R-T). Tak1, a JNKKK, is a known up-regulator of JNK signaling (Geuking et al., 2009; Silverman et al., 2003; Stronach, 2005; Weston and Davis, 2002). When *UAS-Tak^{1}* was expressed using a single copy of *sev-GAL4* diver, all progenies (N = 500) eclosed with a bar-like eye. However, driving *UAS-tak^{1}* with two copies of *sev-GAL4*, which would elevate JNK activity much more, caused death of all progeny (N = 500) at early pupal stage similar to *GMR-GAL4>UAS-Tak^{1}*.

To further confirm enhanced JNK signaling and consequent Dilp8 activity, we measured levels of transcripts of the JNK pathway gene *gadd45*, and *dilp8* in late larval and early pupal *GMR-GAL4>UAS-GFP*, *GMR-GAL4>UAS-Ras^{V12}*, *GMR-GAL4>UAS-tak^{1}* and *GMR-GAL4>UAS-127Q* eye discs. In agreement with the absence of pupal death in *GMR-GAL4>UAS-127Q*, neither *dilp8* nor *gadd45* transcripts showed any appreciable change when compared to *GMR-GAL4>UAS-GFP* control. On the other hand, the early dying *GMR-GAL4>UAS-Ras^{V12}* and *GMR-GAL4>UAS-tak^{1}* individuals showed more abundant *dilp8* transcripts at pupal than at larval stages (Fig. 8O). The *gadd45* transcripts also showed significant increase in *GMR-GAL4>UAS-tak^{1}* early pupal eye discs (Fig. 8O).

We examined if increased Ras and JNK activity in wing discs also caused early pupal lethality. We used *MS1096-GAL4* to drive *UAS-Ras^{V12}*, *UAS-tak^{1}*, or *UAS-rpr* expression in the wing pouch region (Capdevila and Guerrero, 1994). *MS1096-GAL4* driven expression of activated Ras caused near complete (~99%, N=500) early pupal lethality, while that of *UAS-tak^{1}* led to about 60% (N=500) death at early pupal stage; some died as late pupa while only ~15% eclosed with thoracic defects and nearly-absent wings. Unlike *GMR-GAL4>UAS-rpr*, *MS1096-GAL4>UAS-rpr* expression did not cause early pupal death. However, about 60% (N=200) of them died as late pupae while 40% eclosed with vestigial wings. Wing discs of 8-9 Hr old *MS1096-GAL4>UAS-Ras^{V12}* and *MS1096-GAL4 UAS-tak^{1}* pupae showed very high *dilp8* while the *ptth* transcripts in same age pupal brain were reduced (Supplementary Fig. S5), more so in *MS1096-GAL4>UAS-Ras^{V12}*. Although *MS1096-GAL4>UAS-rpr* too showed increased *dilp8* and reduced

ptth levels, they were far less pronounced than in *MS1096-GAL4>UAS-Ras*^{V12} or *MS1096-GAL4 UAS-tak*^{1} (Supplementary Fig. S5), which correlates with their survival through the early pupal period.

A summary of pupal survival, p-JNK and Dilp8 levels in the different genotypes examined in our study is presented in Table 2, which shows that both the JNK and Dilp8 signaling cascades were up-regulated in larval and early pupal eye discs, respectively, in all the genotypes that displayed high death at about 23-25 Hr APF.

Table 2. High p-JNK and Dilp8 in larval and pupal imaginal disks correlate with early pupal lethality

Genotype	**Pupal survival (N=500 or more for each genotype)**	**p-JNK levels in 3rd instar & early pupal eye discs (relative to control expressing only *UAS-GFP*)**	**Dilp8 levels in early pupal eye discs and brain lobes**
		Eye disc	**Eye disc**
1. *GMR-GAL4>UAS-Ras1*^{V12}	100% Early pupal death	Very high	High
2. *GMR-GAL4>UAS-rpr*	100% Early pupal death	Very High	High
3. *GMR-GAL4>UAS-tak*^{1}	100% Early pupal death	Very high	High
4. *GMR-GAL4>UAS-127Q*	100% fly emergence	Normal	Normal
5. *sev-GAL4>UAS-GFP*	100% fly emergence	Normal	Normal
6. *sev-GAL4>UAS-Ras1*^{V12}	88% Late pupal death; 12 % fly emergence	Moderately high	Normal
7. *sev-GAL4>UAS-Ras1*^{V12} *hsrω-RNAi*	96% Early pupal death; 4% late pupal death ((Ray and Lakhotia, 2017))	Very high	High
8. *sev-GAL4>UAS-Ras1*^{V12} *EP3037*	42% Early pupal death; 58% late pupal death ((Ray and Lakhotia, 2017)	High	High
9. *sev-GAL4>RAFRBDFLAG*	100% fly emergence	Low	Not examined
10. *sev-GAL4>UAS-Ras1*^{V12} *RAFRBDFLAG*	100% fly emergence	Low	Not examined
11. *sev-GAL4>UAS-Ras1*^{V12} *RAFRBDFLAG hsrω-RNAi*	100% fly emergence	Low	Not examined
12. *sev-GAL4>UAS-Ras1*^{V12} *RAFRBDFLAGEP3037*	100% fly emergence	Low	Not examined
13. *MS1096-GAL4> UAS-GFP*	100% fly emergence	Not examined but expected normal	Normal
14. *MS1096-GAL4> UAS- Ras1*^{V12}	99% early pupal lethality	Not examined, high expected	High
15. *MS1096-GAL4> UAS- UAS-tak*^{1}	60% early and 25% late pupal lethality	Not examined, high expected	High
16. *MS1096-GAL4> UAS- UAS-rpr*	No early pupal lethality but 60% late pupal lethality	Not examined	Slightly elevated

Shaded cells indicate correlation between early pupal death and very high p-JNK and Dilp8 levels in larval eye discs

4. Discussion

Present study examines possible reasons for the unexpected pupal death following the predominantly eye disc specific *GMR-GAL4* or *sev-GAL4* driven expression of certain transgenes. Early dying pupae lack the early metamorphic changes, which correlated with absence of the normal ecdysone surge occurring after 8-12 Hr APF (Handler, 1982). In

agreement with our hypothesis that the reduced ecdysone leads to early pupal death, we found similar early pupal death following conditional inhibition of ecdysone synthesis during early pupal stage in the temperature sensitive *ecd*^{1} mutant, and that such early pupal deaths could be significantly suppressed by exogenous ecdysone provided during the 8 to 20 Hr interval APF.

In agreement with the reduced levels of ecdysone in pupae, our microarray and qRT-PCR data showed that key genes like *spookier* and *phantom*, involved in ecdysone biosynthesis, are indeed down-regulated in early pupal, but not late third instar stage, prothoracic glands in genotypes showing early pupal death. Together, our findings clearly indicate that the reduced ecdysone titer after the 8-12 Hr APF stage in these genotypes is responsible for the early pupal death. The observed unaltered levels of the *shade* gene transcripts, which encode Cyp314a1 that adds a hydroxyl group to ecdysone in the final step (Huang et al., 2008), may not be relevant in present context since its substrate, ecdysone, would be limiting due to down-regulated *spookier*, *phantom* and *shadow* transcripts in *sev-GAL4>UAS-Ras1*^{V12} *hsrω-RNAi* and *sev-GAL4>UAS-Ras1*^{V12} *EP3037* genotypes. Moreover, *shade* gene product converts ecdysone to 20-hydroxy-ecdysone in fat bodies (Huang et al., 2008). The observed elevation in levels of *disembodied* transcripts (Supplementary Table S2) in the total pupal RNA may appear incongruent, since Disembodied acts between Spookier and Phantom in ecdysone synthesis and, therefore, was expected to be down-regulated. However, the microarray data is derived from total pupal RNA rather than from only the prothoracic glands. Further, *disemodied* is regulated independent of *spookier* (Komura-Kawa et al., 2015), and thus it may express in some other tissues also.

Since CNS derived neuro-endocrine signals regulate ecdysone synthesis and release from prothoracic gland (Henrich et al., 1987a; Niwa and Niwa, 2014), possibility exists that ectopic expression of the *sev-GAL4* and *GMR-GAL4* drivers in certain neurons in brain and ventral ganglia (Ray and Lakhotia, 2015) may directly affect ecdysone synthesis. However, our results that the *sev-GAL4* and *GMR-GAL4* expressing CNS neurons persist when ecdysone synthesis in prothoracic glands was conditionally inhibited using the temperature sensitive *ecd*^{1} mutant allele (Claudius et al., 2014; Henrich et al., 1987b) but disappeared in individuals escaping early death by exogenous ecdysone indicate that persistence of GFP expression in these CNS neurons in the early dying pupae is a consequence, rather than a cause, of the reduced ecdysone signaling.

Further support for the primary role of eye discs in early pupal death in *sev-GAL4>UAS-Ras1*^{V12} *hsrω-RNAi* or *sev-GAL4>UAS-Ras1*^{V12} *EP3037* genotypes is provided by their identical expression in CNS but different in eye discs (Ray and Lakhotia, 2015). While the *GMR-GAL4* is expressed more extensively in nearly all cells posterior to the morphogenetic furrow, the *sev-GAL4* driver expresses only in a subset of photoreceptos (Bowtell et al., 1991; Firth et al., 2006; Freeman, 1996; Maixner et al., 1998; Ray and Lakhotia, 2015). Ectopic expression of activated Ras disrupts development of eye discs (Karim et al., 1996) and like earlier studies (Firth et al., 2006; Karim et al., 1996; Maixner et al., 1998), we also found (Ray and Lakhotia, 2017) more severely affected eyes in *GMR-GAL4>UAS-Ras1*^{V12}. Further, unlike in discs expressing only *sev-GAL4>UAS-Ras1*^{V12}, co-expression of *sev-GAL4>UAS-Ras1*^{V12} with *hsrω-RNAi* or *EP3037*

results in significantly enhanced Ras expression which spreads non-autonomously to neighbouring cells to a much greater extent (Ray and Lakhotia, 2017). Consequently, the cumulative effect of activated Ras expression in these genotypes becomes nearly as strong as in *GMR-GAL4>UAS-Ras1*^{V12} eye discs. Moreover, unlike the imaginal discs, the CNS did not show enhanced p-MAPK or JNK activity in genotypes dying as early pupae. Early pupal death following expression of *UAS-Ras1*^{V12} or *UAS- UAS-tak*^{1} under the wing-disc specific *MS1096-GAL4* driver also confirms the damage in imaginal discs to be the primary source for signals that disrupt early pupal ecdysone surge.

The signal peptide Dilp8 secreted by damaged or abnormally growing imaginal discs plays a significant role in coordinating imaginal tissue growth and ecdysone synthesis in prothoracic gland (Andersen et al., 2015; Colombani et al., 2012; Demay et al., 2014; Garelli et al., 2012; Katsuyama et al., 2015). The enhanced levels of Dilp8 in early pupal peripodial cells in all genotypes that exhibited early pupal death strongly indicate that *GMR-GAL4* or *sev-GAL4 or MS1096-GAL4* driven expression of different transgenes and the consequent disrupted eye or wing disc development triggers Dilp8 synthesis and its secretion by peripodial cells.

Larval or pupal stage lethality was not seen following *tubulin* promoter driven global over-expression of Dilp8A (Vallejo et al., 2015). The absence of death in this case may be because the *tubulin* promoter did not enhance Dilp8 to the required threshold level. Alternatively, and more likely, since a global expression of Dilp8 does not differentially affect different organs, lethality does not ensue, rather the adults become overweight because of equal effect on every tissue, (Vallejo et al., 2015). Our experimental conditions disrupt development of only specific cell types and thus are expected to activate Dilp8 signaling.

It is reported earlier (Colombani et al., 2012; Demay et al., 2014; Garelli et al., 2012; Garelli et al., 2015; Katsuyama et al., 2015; Zimmermann et al., 2015) that damage to developing discs activates JNK signaling which in turn activates Dilp8. Activated Ras is well known to trigger Eiger (TNF) mediated JNK signaling (Andersen et al., 2015; Jones et al., 2016; Khoo et al., 2013; Miles et al., 2011; Minden et al., 1994; Ohsawa et al., 2012; Uhlirova et al., 2005; Wu et al., 2010). The complete nullification of the activated Ras effects by co-expression of RafRBDFLAG, a dominant negative suppressor of Ras signaling (Freeman et al., 2010), further confirmed that the elevated Ras-signaling mediated damage to imaginal discs indeed triggered the JNK signaling seen in our microarray, qRT-PCR and immunostaining data. It is interesting that while *tak*^{1} transcript levels, whose product specifically activates JNK pathway (Takatsu et al., 2000) were not affected in any of the genotypes examined, those of its homolog *takl1* (Manning et al., 2002) were highly up-regulated in *sev-GAL4>UAS-Ras1*^{V12} *hsrω-RNAi* and *sev-GAL4>UAS-Ras1*^{V12} *EP3037* pupae, which may contribute to the observed elevated JNK signaling in these eye discs. Our findings that all the genotypes that show early pupal lethality had elevated p-JNK levels in eye or wing discs and elevated Dilp8 in early pupal discs (Table 2) reinforce involvement of JNK signaling in the process of Dilp8 synthesis. Our results for the first

time indicates that out of many players of JNK signaling pathway Eiger, Gadd45 and Tak1-like 1 may play major role in regulating Dilp8 synthesis in imaginal discs.

Ptth triggers prothoracic gland to synthesize ecdysone hormone (McBrayer et al., 2007; Rewitz et al., 2009; Yamanaka et al., 2013). The observed reduction in *ptth* transcript levels in brain lobes of early dying pupae following the higher Dilp8 secreted by early pupal imaginal discs results in reduced ecdysone synthesis in prothoracic glands. Dlip8 is reported to delay Ptth synthesis via the Lgr3 receptor (Colombani et al., 2015; Colombani et al., 2012; Garelli et al., 2012; Vallejo et al., 2015). In this context, the presence of high levels of Dilp8 in the four pairs of cerebral neurons in 8-9 Hr old pupa, whose axons project on proximal region of prothoracic gland and the reduction in transcripts of Lgr3 receptors in brain lobes of early dying pupae is intriguing. Presence of Dilp8 protein in these neurons may be a normal developmental expression because of the identical pattern seen even in the absence of *sev-GAL4* driven activated Ras expression. It remains to be seen if the Dilp8 positive neurons in our study are also expressing Lgr3. Reasons for the reduction in the *lgr3* transcripts in brain lobes of early dying pupae are not clear but may reflect a negative feedback loop activated by enhanced Dilp8 signaling. Another intriguing observation was the presence of *dilp8* transcripts in brain and ventral ganglia of all genotypes and their elevation in early dying pupae. Although Dilp8 signal peptide is reportedly produced by imaginal discs (Colombani et al., 2012; Garelli et al., 2012), the modENcode mRNA tissue seq and cell line seq data at the Flybase report a low expression of *dilp8* transcripts in CNS of third instar larvae and P8 pupal stage like that in normal larval imaginal discs (http://flybase.org/report/Fbgn0036690.html). The elevated *dilp8* transcripts in brain lobes without a parallel increase in Dilp8 protein in the early dying pupae may reflect post-transcriptional regulation of *dilp8* expression (Jones et al., 2015).

Together, our results show that the elevated JNK signaling in late larval eye discs, either due to ectopically expressed high levels of activated Ras or Reaper or Tak1, leads them to secret more Dilp8 after pupariation. The early pupal death following elevated levels of Dilp8 in eye or wing discs observed in our study is novel since earlier studies (Colombani et al., 2012; Demay et al., 2014; Garelli et al., 2012; Garelli et al., 2015; Katsuyama et al., 2015; Zimmermann et al., 2015) suggested a major role of Dilp8 in delaying late larval ecdysone synthesis to let them attain minimal growth and development before the pupal stage. Unlike the earlier reported nearly 100 fold increase in Dilp8 transcript levels in larvae expressing mutant polarity or tumor inducing genes (Bunker et al., 2015; Figueroa-Clarevega and Bilder, 2015), we found much less-fold increase in *dilp8* transcripts in late larval discs in genotypes that show early pupal death. On the other hand, the very high Dilp8 levels in the early pupal eye discs of early dying pupal genotypes correlates with the substantial reduction in transcripts of *ptth* in brain and of some Halloween genes in pupal prothoracic glands. Therefore, it appears that the damage caused by *GMR-GAL4* or *sev-GAL4* or *MS1096-GAL4* driven expression of the specific transgenes that elevate JNK signaling during the 3rd instar stage remains below the threshold required for significantly elevating Dilp8 secretion. Consequently the larva pupates as usual. However, as the *GAL4* driven damage and the consequent increase in JNK signaling continues, and spreads non-cell-

autonomously, Dilp8 levels increase following pupation and suppress the next ecdysone release in >8-9 Hr pupae. Since at this stage, organism cannot postpone development, death ensues.

5. Conclusions

Our study reveals that pupal death following predominantly eye-specific *GMR-GAL4* or *sev-GAL4* or wing-specific *MS1096-GAL4* driven over-expression of activated Ras or JNK signaling component is because of activation of the JNK-mediated Dilp8 secretion by imaginal discs, which lowers PTTH in brain and thus inhibits ecdysone synthesis in prothoracic glands following pupariation. Present study highlights the inter-organ communication between epithelia and the CNS and other organs. Whereas earlier studies focused more on how a tumorous or damaged imaginal disc in third instar larvae enhanced Dilp8 expression to delay pupation, our study emphasizes that disturbance in Ras-JNK signaling pathway and consequent downstream events in imaginal disc cells regulates Dlip8-Ptth-ecdysone axis even at the post-pupariation stage.

Material and Methods

Fly stocks

All fly stocks and crosses were maintained on standard agar cornmeal medium at 24±1^{0}C. The following stocks were obtained from the Bloomington *Drosophila* Stock Centre (USA): w^{1118}; *sev-GAL4* (no. 5793), w^{1118}; *UAS-GFP* (no. 1521), w^{1118}; *UAS-rpr* (no. 5824), w^{1118}; *UAS-tak1* (no. 58810), *ecd*^{1} (no. 218) and w^{1118}; *UAS-Ras1*^{V12} (no. 4847). The other stocks, viz., w^{1118}; *GMR-GAL4* (Freeman, 1996), w^{1118} *MS1096* (Capdevila and Guerrero, 1994); w^{1118}; *UAS-hsrω-RNAi*^{3} (Mallik and Lakhotia, 2009b), w^{1118}; *EP3037/TM6B* (Mallik and Lakhotia, 2009b), w^{1118}; *GMR-GAL4; UAS-hsrω-RNAi*^{3}, w^{1118}; *GMR-GAL4; EP3037/TM6B*, w^{1118}; *Sp/CyO; dco*^{2} *e/TM6B* and w^{1118}; *UAS-127Q* (Kazemi-Esfarjani and Benzer, 2000), were available in the laboratory. The *UAS-hsrω-RNAi*^{3} is a transgenic line for down regulating the hsrω-nuclear transcripts while the *EP3037* allele over-expresses *hsrω* gene under a GAL4 driver (Mallik and Lakhotia, 2009b). The *UAS-RafRBDFLAG* stock (Freeman et al., 2010) was provided by Dr S Sanyal (Emory University, USA). Using these stocks, appropriate crosses were made to generate following stocks:

a) w^{1118}; *sev-GAL4 UAS-GFP; dco*^{2} *e/TM6B*
b) w^{1118}; *sev-GAL4 UAS-GFP; UAS-hsrω-RNAi*^{3}
c) w^{1118}; *sev-GAL4 UAS-GFP; EP3037/TM6B*
d) w^{1118}; *UAS-GFP; UAS-Ras1*^{V12}
e) w^{1118}; *sev-GAL4 UAS-GFP; ecd*^{1}
f) w^{1118}; *UAS-RafRBDFLAG; UAS-Ras1*^{V12}*/TM6B*

Some of these were used directly or were further crossed to obtain progenies of following genotypes as required:

a) w^{1118}; sev-GAL4 *UAS-GFP/UAS-GFP;* dco^2 *e/+*
b) w^{1118}; *sev-GAL4 UAS-GFP/UAS-GFP;* dco^2 *e/UAS-Ras1*^{V12}
c) w^{1118}; *sev-GAL4 UAS-GFP/UAS-GFP; UAS-hsrω-RNA*$^{i3/}$*UAS-Ras1*^{V12}
d) w^{1118}; *sev-GAL4 UAS-GFP/UAS-GFP; EP3037/ UAS-Ras1*^{V12}
e) w^{1118}; sev-GAL4 *UAS-GFP/UAS-RafRBDFLAG;* dco^2 *e/+*
f) w^{1118}; *sev-GAL4 UAS-GFP/UAS-RafRBDFLAG;* dco^2 *e/UAS-Ras1*^{V12}
g) w^{1118}; *sev-GAL4 UAS-GFP/UAS-RafRBDFLAG; UAS-hsrω-RNAi*^{3}*/UAS-Ras1*^{V12}
h) w^{1118}; *sev-GAL4 UAS-GFP/UAS-RafRBDFLAG; EP3037/UAS-Ras1*^{V12}
i) w^{1118}; *GMR-GAL4/UAS-GFP*
j) w^{1118};*GMR-GAL4/UAS-GFP; +/ UAS-Ras1*^{V12}
k) w^{1118};*GMR-GAL4/UAS-GFP; UAS-hsrω-RNAi*^{3}*/ UAS-Ras1*^{V12}
l) w^{1118};*GMR-GAL4/UAS-GFP; EP3037/ UAS-Ras1*^{V12}
m) w^{1118}; *GMR-GAL4/UAS-rpr*
n) w^{1118}; *GMR-GAL4/+;+/UAS-Tak1*
o) w^{1118}; *GMR-GAL4/UAS-127Q;+/+*
p) w^{1118} *MS1096*
q) w^{1118} *MS1096;+/UAS-rpr;+/+*
r) w^{1118} *MS1096; +/+;+/UAS-Tak1*
s) w^{1118} *MS1096; +/+;+/ UAS-Ras1*^{V12}

The w^{1118}, dco^2 *e* and *UAS-GFP* markers are not mentioned while writing genotypes in Results while the *UAS-hsrω-RNAi*^{3} transgene (Mallik and Lakhotia, 2009b) is referred to as *hsrω-RNAi*.

For conditional inhibition of ecdysone synthesis using the temperature-sensitive ecd^1 mutant allele (Henrich et al., 1987b), freshly formed *sev-GAL4 UAS-GFP;* ecd^1 0-1 Hr pupae, reared from egg-laying till pupation at 24±1^{0}C, were transferred to 30±1^{0}C for further development.

Flies of desired genotypes were crossed and their progeny eggs were collected at hourly intervals. Larvae that hatched during a period of 1 Hr were separated to obtain sync Hronously growing larvae. Likewise, larvae that began pupation during an interval of 1 Hr were separated to obtain pupae of defined age (expressed as Hr after pupa formation or Hr APF).

GFP imaging

Actively moving late third instar larvae and pupae of desired ages were dissected in Poels' salt solution (PSS) (Tapadia and Lakhotia, 1997) and tissues fixed in 4% paraformaldehyde (PFA) in phosphate-buffered saline (PBS, 130 mm NaCl, 7 mm Na_2HPO_4, 3mm KH_2PO_4,pH 7.2) for 20 min. After t Hree 10 min washes in 0.1% PBST (PBS + 0.1% Triton-X-100), the tissues were counterstained with DAPI (4', 6-diamidino-2-phenylindole dihydrochloride, 1µg/ml) and mounted in DABCO for imaging the *sev-GAL4* or *GMR-GAL4* driven *UAS-GFP* expression.

Whole organ immunostaining

Brain and eye discs from *sev-GAL4 UAS-GFP/UAS-GFP;* dco^2*e/+, sev-GAL4 UAS-GFP/UAS-GFP;* dco^2 *e/UAS-Ras1*^{V12}*,sev-GAL4 UAS-GFP/UAS-GFP; UAS-hsrω-RNAi/UAS-Ras1*^{V12}*,* and

sev-GAL4 UAS-GFP/UAS-GFP; and *EP3037/UAS-Ras1^{V12}* actively migrating late third instar larvae and pupae of desired age were dissected in PSS and immediately fixed in freshly prepared 4% paraformaldehyde in PBS for 20 min and processed for immunostaining as described earlier (Prasanth et al., 2000). The primary antibodies used were: mouse monoclonal anti-Broad-core (1:50; DSHB, 25E9.D7), rabbit monoclonal anti-p-JNK (1:100; Promega) at and rat anti-Dilp8 (1:50; gifted by Dr. P. Léopold, France) (Colombani et al., 2012). Appropriate secondary antibodies conjugated either with Cy3 (1:200, Sigma-Aldrich, India) or Alexa Fluor 633 (1:200; Molecular Probes, USA) or Alexa Fluor 546 (1:200; Molecular Probes, USA) were used to detect the given primary antibody. C Hromatin was counterstained with DAPI (4', 6-diamidino-2-phenylindole dihydrochloride, 1µg/ml). Tissues were mounted in DABCO antifade mountant (Sigma) for confocal microscopy with Zeiss LSM Meta 510 using Plan-Apo 40X (1.3-NA) or 63X (1.4-NA) oil immersion objectives. Quantitative estimates of the proteins in different regions of eye discs were obtained with the help of Histo option of the Zeiss LSM Meta 510 software. All images were assembled using the Adobe Photoshop 7.0 software.

Measurement of ecdysone levels

Fifteen pupae of the desired stages and genotypes were collected in 1.5 ml tubes and stored at -70°C in methanol till further processing. They were homogenized in methanol and centrifuged at 13000 rpm following which the pellets were re-extracted in ethanol and air dried (Ou et al., 2011). The dried extracts were dissolved in EIA buffer at 4°C overnight prior to the enzyme immunoassay. The 20E-EIA antiserum (#482202), 20E AChE tracer (#482200), precoated (Mouse Anti-Rabbit IgG) EIA 96-Well Plates (#400007), and Ellman's Reagent (#400050) were obtained from Cayman Chemical (USA), and the ecdysone assay was performed according to the manufacturer's instructions.

Microarray Analysis

RNA was isolated from 16-17 Hr old *sev-GAL4>UAS-GFP*, *sev-GAL4>UAS-Ras1^{V12}*, *sev-GAL4>UAS-Ras1^{V12} hsrω*-RNAi and *sev-GAL4>UAS-Ras1^{V12} EP3037* pupae using TriReagent (Sigma-Aldrich) as per manufacturer's instructions. Microarray analysis of these RNA samples was performed on Affimetrix Drosophila Genome 2.0 microarray chips for 3' IVT array following the Affymetrix GeneChip Expression Analysis Technical manual using the GeneChip 3' IVT Plus Reagent Kit, Affymetrix GeneChip® Fluidics station 450, GeneChip® Hybridization oven 645 and GeneChip®Scanner 3000. Summary of the expression levels for each gene in the four genotypes was obtained from the Affymetrix Transcription analysis console and was subjected to Gene ontology search using David Bioinformatics software (https://**david**.ncifcrf.gov).The microarray data have been deposited at GEO repository (http://www.ncbi.nlm.nih.gov/geo/query/acc.cgi?acc=GSE80703).

Real Time Quantitative Reverse transcription–PCR (qRT-PCR)

Total RNAs were isolated from eye discs and brain ganglia of third instar larvae and appropriate pupal stages of the desired genotypes using TriReagent as per the manufacturer's (Sigma-

Aldrich) instructions. First-strand cDNAs were synthesized as described earlier (Mallik and Lakhotia, 2009b). The prepared cDNAs were subjected to real time PCR using forward and reverse primer pairs as listed in Supplementary Table S3. Real time qPCR was performed using 5µl qPCR Master Mix (Syber Green, Thermo Scientific), 2 picomol/µl of each primer per reaction in 10 µl of final volume in ABI 7500 Real time PCR machine.

Acknowledgements

We thank the Bloomington *Drosophila* Stock Center (USA) for providing fly stocks, Developmental Studies Hybridoma Bank (DSHB, Iowa, USA) for the anti-Broad-Core and Dr. P. Leopold (France) for the anti-Dilp8. We thank the DBT-BHU Interdisciplinary School of Life Sciences for the Microarray and real time PCR facilities.

Competing interests

Authors declare no conflicting interests

Author contributions

MR and SCL planned experiments, analyzed results and wrote the manuscript. MR carried out the experimental work and collected data.

Funding

This work was supported by a research grant (no. BT/PR6150/COE/34/20/2013) to SCL by the Department of Biotechnology, Ministry of Science and Technology, Govt. of India, New Delhi. SCL was also supported by the Raja Ramanna Fellowship of the Department of Atomic Energy, Govt. of India, Mumbai and is currently supported as Senior Scientist by the Indian National Science Academy (New Delhi). MR was supported by the Council of Scientific & Industrial Research, New Delhi t through a senior research fellowship.

Data availability

The microarray data have been deposited at GEO repository (http://www.ncbi.nlm.nih.gov/geo/query/acc.cgi?acc=GSE80703).

References

Andersen, D. S., Colombani, J., Palmerini, V., Chakrabandhu, K., Boone, E., Röthlisberger, M., Toggweiler, J., Basler, K., Mapelli, M. and Hueber, A.-O. (2015). The Drosophila TNF receptor Grindelwald couples loss of cell polarity and neoplastic growth. *Nature* **522**, 482-486.

Bowtell, D. D., Lila, T., Michael, W. M., Hackett, D. and Rubin, G. M. (1991). Analysis of the enhancer element that controls expression of sevenless in the developing Drosophila eye. *Proc Natl Acad Sci U S A* **88**, 6853-7.

Bunker, B. D., Nellimoottil, T. T., Boileau, R. M., Classen, A. K. and Bilder, D. (2015). The transcriptional response to tumorigenic polarity loss in Drosophila. *Elife* **4**, e03189.

Capdevila, J. and Guerrero, I. (1994). Targeted expression of the signaling molecule decapentaplegic induces pattern duplications and growth alterations in Drosophila wings. *The EMBO journal* **13**, 4459-4468.

Claudius, A.-K., Romani, P., Lamkemeyer, T., Jindra, M. and Uhlirova, M. (2014). Unexpected role of the steroid-deficiency protein ecdysoneless in pre-mRNA splicing. *PLoS Genet* **10**, e1004287.

Colombani, J., Andersen, D. S., Boulan, L., Boone, E., Romero, N., Virolle, V., Texada, M. and Léopold, P. (2015). Drosophila Lgr3 couples organ growth with maturation and ensures developmental stability. *Current Biology* **25**, 2723-2729.

Colombani, J., Andersen, D. S. and Léopold, P. (2012). Secreted peptide Dilp8 coordinates Drosophila tissue growth with developmental timing. *Science* **336**, 582-585.

Demay, Y., Perochon, J., Szuplewski, S., Mignotte, B. and Gaumer, S. (2014). The PERK pathway independently triggers apoptosis and a Rac1/Slpr/JNK/Dilp8 signaling favoring tissue homeostasis in a chronic ER stress Drosophila model. *Cell death & disease* **5**, e1452.

Emery, I. F., Bedian, V. and Guild, G. M. (1994). Differential expression of Broad-Complex transcription factors may forecast tissue-specific developmental fates during Drosophila metamorphosis. *Development* **120**, 3275-3287.

Figueroa-Clarevega, A. and Bilder, D. (2015). Malignant Drosophila tumors interrupt insulin signaling to induce cachexia-like wasting. *Developmental Cell* **33**, 47-55.

Firth, L. C., Li, W., Zhang, H. and Baker, N. E. (2006). Analyses of RAS regulation of eye development in Drosophila melanogaster. *Methods in enzymology* **407**, 711-721.

Freeman, A., Bowers, M., Mortimer, A. V., Timmerman, C., Roux, S., Ramaswami, M. and Sanyal, S. (2010). A new genetic model of activity-induced Ras signaling dependent pre-synaptic plasticity in Drosophila. *Brain research* **1326**, 15-29.

Freeman, M. (1996). Reiterative use of the EGF receptor triggers differentiation of all cell types in the Drosophila eye. *Cell* **87**, 651-60.

Garelli, A., Gontijo, A. M., Miguela, V., Caparros, E. and Dominguez, M. (2012). Imaginal discs secrete insulin-like peptide 8 to mediate plasticity of growth and maturation. *Science* **336**, 579-582.

Garelli, A., Heredia, F., Casimiro, A. P., Macedo, A., Nunes, C., Garcez, M., Dias, A. R. M., Volonte, Y. A., Uhlmann, T. and Caparros, E. (2015). Dilp8 requires the neuronal relaxin receptor Lgr3 to couple growth to developmental timing. *Nature communications* **6**, 8732.

Geuking, P., Narasimamurthy, R., Lemaitre, B., Basler, K. and Leulier, F. (2009). A non-redundant role for Drosophila Mkk4 and hemipterous/Mkk7 in TAK1-mediated activation of JNK. *PloS one* **4**, e7709.

Handler, A. M. (1982). Ecdysteroid titers during pupal and adult development in Drosophila melanogaster. *Dev Biol* **93**, 73-82.

Hauling, T., Krautz, R., Markus, R., Volkenhoff, A., Kucerova, L. and Theopold, U. (2014). A Drosophila immune response against Ras-induced overgrowth. *Biology open*, BIO20146494.

Henrich, V. C., Pak, M. D. and Gilbert, L. I. (1987a). Neural factors that stimulate ecdysteroid synthesis by the larval ring gland ofDrosophila melanogaster. *Journal of Comparative Physiology B* **157**, 543-549.

Henrich, V. C., Tucker, R. L., Maroni, G. and Gilbert, L. I. (1987b). The ecdysoneless (ecd1ts) mutation disrupts ecdysteroid synthesis autonomously in the ring gland of Drosophila melanogaster. *Developmental biology* **120**, 50-55.

Huang, X., Warren, J. T. and Gilbert, L. I. (2008). New players in the regulation of ecdysone biosynthesis. *Journal of Genetics and Genomics* **35**, 1-10.

Jones, C. I., Pashler, A. L., Towler, B. P., Robinson, S. R. and Newbury, S. F. (2015). RNA-seq reveals post-transcriptional regulation of Drosophila insulin-like peptide dilp8 and the neuropeptide-like precursor Nplp2 by the exoribonuclease Pacman/XRN1. *Nucleic acids research* **44**, 267-280.

Jones, C. I., Pashler, A. L., Towler, B. P., Robinson, S. R. and Newbury, S. F. (2016). RNA-seq reveals post-transcriptional regulation of Drosophila insulin-like peptide dilp8 and the neuropeptide-like precursor Nplp2 by the exoribonuclease Pacman/XRN1. *Nucleic acids research* **44**, 267-280.

Karim, F. D., Chang, H. C., Themen, M., Wassarman, D. A., Laverty, T. and Rubin, G. M. (1996). A screen for genes that function downstream of Ras1 during Drosophila eye development. *Genetics* **143**, 315-329.

Katsuyama, T., Comoglio, F., Seimiya, M., Cabuy, E. and Paro, R. (2015). During Drosophila disc regeneration, JAK/STAT coordinates cell proliferation with Dilp8-mediated developmental delay. *Proceedings of the National Academy of Sciences* **112**, E2327-E2336.

Kazemi-Esfarjani, P. and Benzer, S. (2000). Genetic suppression of polyglutamine toxicity in Drosophila. *Science* **287**, 1837-1840.

Khoo, P., Allan, K., Willoughby, L., Brumby, A. M. and Richardson, H. E. (2013). In Drosophila, RhoGEF2 cooperates with activated Ras in tumorigenesis through a pathway involving Rho1–Rok–Myosin-II and JNK signalling. *Disease Models and Mechanisms* **6**, 661-678.

Komura-Kawa, T., Hirota, K., Shimada-Niwa, Y., Yamauchi, R., Shimell, M., Shinoda, T., Fukamizu, A., O'Connor, M. B. and Niwa, R. (2015). The Drosophila zinc finger transcription factor Ouija board controls ecdysteroid biosynthesis through specific regulation of spookier. *PLoS Genet* **11**, e1005712.

Lakhotia, S. C. (2011). Forty years of the 93D puff of Drosophila melanogaster. *J. Biosciences* **36**, 399-423.

Lakhotia, S. C. (2016). Non-coding RNAs have key roles in cell regulation. *Proc. Indian Natn. Sci. Acad.* **82**, 1171-1182.

Maixner, A., Hecker, T. P., Phan, Q. N. and Wassarman, D. A. (1998). A screen for mutations that prevent lethality caused by expression of activated sevenless and Ras1 in the Drosophila embryo. *Developmental genetics* **23**, 347-361.

Mallik, M. and Lakhotia, S. C. (2009a). The developmentally active and stress-inducible noncoding *hsromega* gene is a novel regulator of apoptosis in *Drosophila*. *Genetics* **183**, 831-852.

Mallik, M. and Lakhotia, S. C. (2009b). RNAi for the large non-coding hsr omega transcripts suppresses polyglutamine pathogenesis in *Drosophila* models. *Rna Biology* **6**, 464-478.

Manning, G., Plowman, G. D., Hunter, T. and Sudarsanam, S. (2002). Evolution of protein kinase signaling from yeast to man. *Trends in biochemical sciences* **27**, 514-520.

Martín-Blanco, E., Gampel, A., Ring, J., Virdee, K., Kirov, N., Tolkovsky, A. M. and Martinez-Arias, A. (1998). puckered encodes a phosphatase that mediates a feedback loop regulating JNK activity during dorsal closure in Drosophila. *Genes & development* **12**, 557-570.

McBrayer, Z., Ono, H., Shimell, M., Parvy, J.-P., Beckstead, R. B., Warren, J. T., Thummel, C. S., Dauphin-Villemant, C., Gilbert, L. I. and O'Connor, M. B. (2007). Prothoracicotropic hormone regulates developmental timing and body size in Drosophila. *Developmental Cell* **13**, 857-871.

Miles, W. O., Dyson, N. J. and Walker, J. A. (2011). Modeling tumor invasion and metastasis in Drosophila. *Disease Models and Mechanisms* **4**, 753-761.

Minden, A., Lin, A., McMahon, M., Lange-Carter, C., Dérijard, B., Davis, R. J., Johnson, G. L. and Karin, M. (1994). Differential activation of ERK and JNK mitogen-activated protein kinases by Raf-1 and MEKK. *Science* **266**, 1719-1723.

Morris, E. J., Michaud, W. A., Ji, J.-Y., Moon, N.-S., Rocco, J. W. and Dyson, N. J. (2006). Functional identification of Api5 as a suppressor of E2F-dependent apoptosis in vivo. *PLoS Genet* **2**, e196.

Nässel, D. R., Kubrak, O. I., Liu, Y., Luo, J. and Lushchak, O. V. (2013). Factors that regulate insulin producing cells and their output in Drosophila. *Frontiers in Physiology* **4**.

Niwa, Y. S. and Niwa, R. (2014). Neural control of steroid hormone biosynthesis during development in the fruit fly Drosophila melanogaster. *Genes & genetic systems* **89**, 27-34.

Ohsawa, S., Sato, Y., Enomoto, M., Nakamura, M., Betsumiya, A. and Igaki, T. (2012). Mitochondrial defect drives non-autonomous tumour progression through Hippo signalling in Drosophila. *Nature* **490**, 547-551.

Ou, Q., Magico, A. and King-Jones, K. (2011). Nuclear receptor DHR4 controls the timing of steroid hormone pulses during Drosophila development. *PLoS Biol* **9**, e1001160.

Prasanth, K., Rajendra, T., Lal, A. and Lakhotia, S. (2000). Omega speckles - a novel class of nuclear speckles containing hnRNPs associated with noncoding hsr-omega RNA in *Drosophila*. *J. Cell Sci.* **113 Pt 19**, 3485-3497.

Ragab, A., Buechling, T., Gesellchen, V., Spirohn, K., Boettcher, A. L. and Boutros, M. (2011). Drosophila Ras/MAPK signalling regulates innate immune responses in immune and intestinal stem cells. *The EMBO journal* **30**, 1123-1136.

Ray, M. and Lakhotia, S. C. (2015). The commonly used eye-specific sev-GAL4 and GMR-GAL4 drivers in Drosophila melanogaster are expressed in tissues other than eyes also. *Journal of genetics* **94**, 407-416.

Ray, M. and Lakhotia, S. C. (2017). Altered hsrω lncRNA levels in activated Ras background further enhance Ras activity in Drosophila eye and induces more R7 photoreceptors. *bioRxiv*, DOI: 10.1101/224543.

Rewitz, K. F., Yamanaka, N., Gilbert, L. I. and O'Connor, M. B. (2009). The insect neuropeptide PTTH activates receptor tyrosine kinase torso to initiate metamorphosis. *Science* **326**, 1403-1405.

Sang, T.-K. and Jackson, G. (2005). Drosophila models of neurodegenerative disease. *NeuroRx : the journal of the American Society for Experimental NeuroTherapeutics* **2**, 438-446.

Silverman, N., Zhou, R., Erlich, R. L., Hunter, M., Bernstein, E., Schneider, D. and Maniatis, T. (2003). Immune activation of NF-κB and JNK requires Drosophila TAK1. *Journal of Biological Chemistry* **278**, 48928-48934.

Stronach, B. (2005). Dissecting JNK signaling, one KKKinase at a time. *Dev Dyn* **232**, 575-84.

Takatsu, Y., Nakamura, M., Stapleton, M., Danos, M. C., Matsumoto, K., O'Connor, M. B., Shibuya, H. and Ueno, N. (2000). TAK1 participates in c-Jun N-terminal kinase signaling during Drosophila development. *Mol Cell Biol* **20**, 3015-26.

Tapadia, M. and Lakhotia, S. (1997). Specific induction of the hsr omega locus of Drosophila melanogaster by amides. *Chromosome Research* **5**, 359-362.

Uhlirova, M., Jasper, H. and Bohmann, D. (2005). Non-cell-autonomous induction of tissue overgrowth by JNK/Ras cooperation in a Drosophila tumor model. *Proceedings of the National Academy of Sciences of the United States of America* **102**, 13123-13128.

Vallejo, D. M., Juarez-Carreño, S., Bolivar, J., Morante, J. and Dominguez, M. (2015). A brain circuit that synchronizes growth and maturation revealed through Dilp8 binding to Lgr3. *Science* **350**, aac6767.

Warren, J. T., Petryk, A., Marqués, G., Jarcho, M., Parvy, J.-P., Dauphin-Villemant, C., O'Connor, M. B. and Gilbert, L. I. (2002). Molecular and biochemical characterization of two P450 enzymes in the ecdysteroidogenic pathway of Drosophila melanogaster. *Proceedings of the National Academy of Sciences* **99**, 11043-11048.

Weston, C. R. and Davis, R. J. (2002). The JNK signal transduction pathway. *Current Opinion in Genetics & Development* **12**, 14-21.

Wu, M., Pastor-Pareja, J. C. and Xu, T. (2010). Interaction between RasV12 and scribbled clones induces tumour growth and invasion. *Nature* **463**, 545-548.

Yamanaka, N., Rewitz, K. F. and O'Connor, M. B. (2013). Ecdysone control of developmental transitions: lessons from Drosophila research. *Annual Review of Entomology* **58**, 497-516.

Zhou, B., Williams, D. W., Altman, J., Riddiford, L. M. and Truman, J. W. (2009). Temporal patterns of broad isoform expression during the development of neuronal lineages in Drosophila. *Neural development* **4**, 1.

Zimmermann, M., Kugler, S. J., Schulz, A. and Nagel, A. C. (2015). Loss of putzig Activity Results in Apoptosis during Wing Imaginal Development in Drosophila. *PloS one* **10**, e0124652.

Zollman, S., Godt, D., Prive, G. G., Couderc, J.-L. and Laski, F. A. (1994). The BTB domain, found primarily in zinc finger proteins, defines an evolutionarily conserved family that includes several developmentally regulated genes in Drosophila. *Proceedings of the National Academy of Sciences* **91**, 10717-10721.